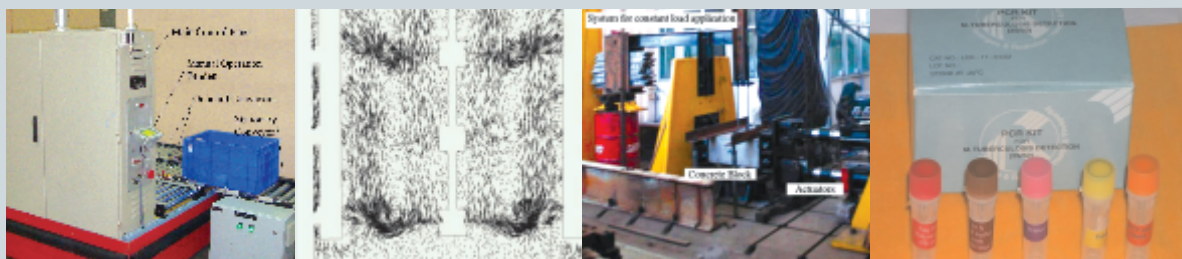




BARC

NEWSLETTER



IN THIS ISSUE

- Organoselenium Compounds: A New Generation of Radioprotectors
- Flow Simulations of Industrial Scale Agitated Tanks
- Experiments on Reinforced Concrete Structures: Sub-Assemblages and Components for Seismic Safety—Post Installed Anchors
- Hollow Fibre Liquid Membranes: A Novel Approach for Nuclear Waste Remediation
- Modeling of Deformation Behaviour of HCP Metals using Crystalplasticity Approach
- A Material Transfer System using Automated Guided Vehicles
- Development of a TB-PCR Kit for the Diagnosis of Tuberculosis

In the Forthcoming Issue

- 1. Multi-Detector Environmental Radiation Monitor with Multichannel Data Communication for Indian Environmental Radiation Monitoring Network (IERMON)**
M. D. Patel et al.
- 2. Characterization of High Level Waste from Reprocessing of PHWR Spent fuel**
B. S. Tomar et al.
- 3. Analytical Performance of Refractometry in Quantitative Estimation of Isotopic Concentration of Heavy Water in Nuclear Reactor**
K. Dhole et al.
- 4. Thermal and Stress Analyses of Oblong Shaped Metallic Melter**
S. M. Thorve et al.
- 5. Development of High Temperature Thermoelectric Materials and Fabrication of Devices**
Deep Prakash et al.
- 6. Mapping Surfaces and Interfaces with Neutrons**
S. Basu
- 7. Development and Fabrication of Superconducting hybrid Cable-In-Conduit-Conductor (CICC) for Indigenous Fusion Programme**
A.K. Singh et al.

Contents

Research Articles

Organoselenium Compounds: A New Generation of Radioprotectors <i>A. Kunwar et al.</i>	1
Flow Simulations of Industrial Scale Agitated Tanks <i>K.K. Singh et al.</i>	8
Experiments on Reinforced Concrete Structures: Sub-Assemblages and Components for Seismic Safety: Post Installed Anchors <i>Akanshu Sharma et al.</i>	16

Technology Development Articles

Hollow Fibre Liquid Membranes: A Novel Approach for Nuclear Waste Remediation <i>S.A. Ansari et al.</i>	23
Modeling of Deformation Behaviour of HCP metals using Crystalplasticity Approach <i>A. Sarkar and J. K. Chakravartty</i>	31
A Material Transfer System using Automated Guided Vehicles <i>R.V. Sakrikar et al.</i>	36
Development of a TB-PCR Kit for the Diagnosis of Tuberculosis <i>Savita Kulkarni et al.</i>	44

News & Events

• Report on 3 rd AONSA Neutron School held at BARC	51
• 55 th DAE Solid State Physics Symposium, (SSPS) 2010: a Report	52
• Report on DAE-BRNS Symposium on Nuclear and Radiochemistry	53
• National Symposium on Advanced Measurement Techniques and Instrumentation (SAMTI-2011): a report	55
• 3 rd DAE-BRNS International Symposium on Material Chemistry; a report	57

BARC Scientists Honoured

Editorial Committee**Chairman**

Dr. V. Venugopal,
Director, RC&I Group

Edited by

Dr. K. Bhanumurthy
Head, SIRD

Associate Editors for this issue

Dr. A.K. Tyagi, CD
Dr. S.K. Mukherjee, FCD

Members

Dr. V. Venugopal, RC&I Group
Mr. C.S.R. Prasad, ChTD
Dr. D.N. Badodkar, DRHR
Dr. A.P. Tiwari, RCnD
Dr. Madangopal Krishnan, MSD
Dr. A.K. Tyagi, CD
Dr. P.V. Varde, RRS
Dr. S.M. Yusuf, SSPD
Mr. Avaneesh Sharma, RED
Dr. C. Srinivas, PsDD
Dr. G. Rami Reddy, RSD
Dr. S.K. Mukherjee, FCD
Mr. G. Venugopala Rao, APPD
Dr. A. Vinod Kumar, EAD
Dr. Anand Ballal, MBD
Dr. K. Bhanumurthy, SIRD
Dr. S.C. Deokattey, SIRD

From the Editor's Desk...

It is our sincere wish to publish quality articles, in diverse R&D areas of our Centre. Sometimes there is a delay in the submission of articles by the authors and at other times there is a delay in the proof corrections of the articles written by them. The process is being streamlined by our Associate Editors and we hope, that the delay period is further reduced, so that the issues are printed fairly on time.

The Founder's Day Special issue will be published in the CD format in the month of October, as was done last year. A general circular will be displayed next month, inviting articles from BARC Scientists and Engineers, who received awards in the year 2010, for their R&D contributions, including the DAE Excellence in Science, Engineering and Technology Awards for the year 2009.

BARC Newsletter has become one of the mediums of expressing our contributions and it is important that all diverse areas are well represented. We request you to contribute articles in unexplored areas and it is our wish that we give priority to publish these articles.

Dr. K. Bhanumurthy
On behalf of the Editorial Committee

Organoselenium Compounds: A New Generation of Radioprotectors

A. Kunwar and K. I. Priyadarsini

Radiation & Photochemistry Division

and

V. K. Jain

Chemistry Division

Abstract

Exposure of living organisms to ionizing radiation can cause health hazards and radioprotectors are employed to minimize such unwanted effects. Over the years a number of sulfhydryl compounds have been examined for radioprotection and only one agent, amifostine, is approved in the clinic. Selenium, a higher analogue of sulfur, is a micronutrient and a constituent of redox enzymes like glutathione peroxidase (GPx). With an aim to develop less toxic, GPx active, organoselenium compounds, as potential radioprotectors, we initiated a programme on synthesis and radioprotection studies of organoselenium compounds. In this article, the current status of research on selenium compounds as radioprotectors is presented.

Radiation exposure and Radioprotectors

Ionizing radiation, both high-energy electromagnetic and charged particles, has a wide spread usage in medicine, agriculture, energy, food storage, etc. and poses health hazards when used improperly. Exposure of living organisms to radiation can induce a number of abnormalities like mutation, cancer, and even death¹. When radiation interacts with living cells, water being the major constituent (~70%), undergoes radiolysis producing highly reactive free radical species, inducing oxidative stress^{1,2}. Cellular damage initiated by these radical species is the origin of tissue and organ injury³. Depending on the type, exposure and linear energy transfer of the radiation, all these events occur within hours to weeks. Sometimes delayed and chronic effects are observable even after many months of exposure.

The extent of radiation injury depends on the absorbed dose, expressed in the units of Gray (Gy), equal to one joule of energy deposition in one kilogram (1 J/kg) of the material. In addition to this, sensitivity of different organs equally determines the

manifestation of radiation injury. For example, organs like brain, bone, muscle, thyroid, pituitary, adrenal and liver are radio-resistant, whereas others like lymphoid organs, reproductive organs, bone marrow and intestinal crypts are radiosensitive¹⁻³. Cellular oxygen enhances the radiation damage and reduced oxygen levels, as observed in certain hypoxic tumors, make them radioresistant².

A radioprotector is a chemical substance or a mixture of compounds, capable of minimizing the damaging effects of ionizing radiation to normal tissue⁴. Development of radioprotectors has been an area of active research from the beginning of the nuclear era. With the recognition that normal tissue protection during radiotherapy is as important as the destruction of the cancer cells, the focus of radioprotection research became more therapy oriented. However, an ideal radioprotector should be able to protect against the deleterious effect of any type of radiation during therapeutic procedures as well as during nuclear accidents. Additionally, a radioprotector should be inexpensive, have no toxic implications, and can be orally administered, with

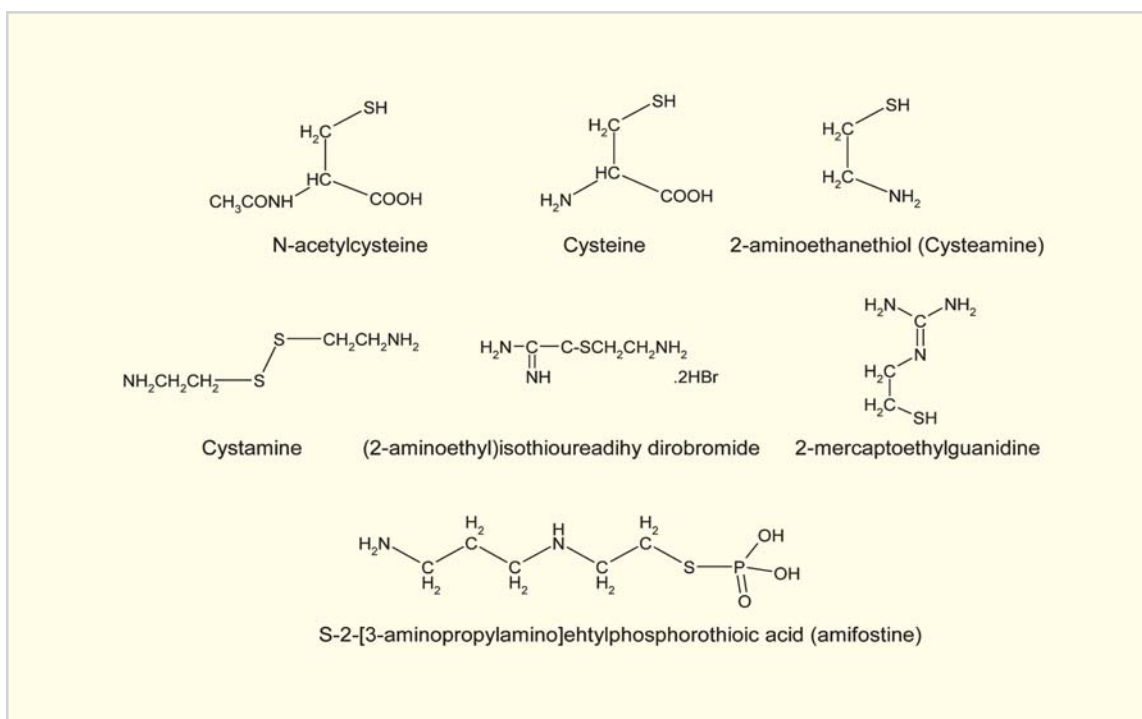
rapid absorption and a reasonably good Dose Modification Factor (DMF). The efficacy of any agent to act as a radioprotector is evaluated in animal models using distinct end-points like survival against radiation-induced lethality, protection to hematopoietic or gastrointestinal (GI) systems, and mutagenesis^{3,4}. The most commonly compared parameter, DMF, varies with the type of radiation, dose rate, administered dosage of radioprotector, time and schedule of treatment, animal strain, etc.

Over the years, several sulfhydryl compounds, such as S-2-[3-aminopropylamino] ethylphosphorothioic acid (amifostine), cysteine, N-acetylcysteine, cysteamine, cystamine, aminoethylisothioureahydrobromide and mercaptoethyl guanidine (scheme 1), have been screened for their radioprotective ability^{3,4}. Out of these, the most effective one, and the only agent approved by the FDA for use in protection of normal tissues in patients treated with radiation is amifostine⁵. It exhibits multiple biochemical properties like free radical scavenging activity and high affinity for DNA.

Although amifostine is a clinically approved radioprotector, its considerable toxicity at radioprotective doses warranted search for effective and non-toxic alternate drugs^{4,6}.

Selenium compounds as antioxidants and radioprotectors

Selenium is an essential trace element for both animals and humans and the recommended nutritional dose of selenium for normal humans is 50–60 $\mu\text{g}/\text{day}$ ⁷. Sodium selenite, selenomethionine, selenium enriched yeast, broccoli, mushrooms, garlic, fish, cabbage, whole grains, wheat, etc. act as selenium supplements. The plants belonging to the genus *astragalus* were found to contain high levels of selenium (several thousand part per million). Selenium deficiency has been implicated in several diseases and some studies have also correlated it with the incidence of cancer. Selenium enters the body through plants, which absorb it from the soil. Inside plants, inorganic selenium is converted to low molecular weight amino acids like selenomethionine (scheme 2). In the body,



Scheme 1: Some selected sulfur compounds used as radioprotectors

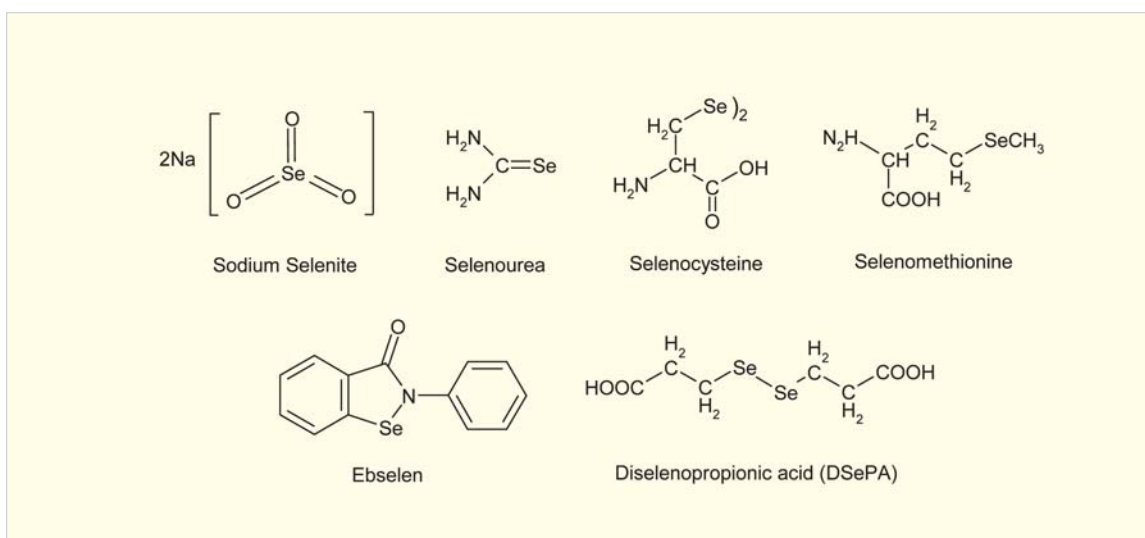
selenomethionine acts as a precursor for the synthesis of selenocysteine, which is the active component of selenoproteins, present in many lineages of life⁷. These proteins are responsible for most of the physiological functions mediated by selenium such as antioxidative action, redox regulation, immune function, etc. In humans, at least 25 selenoproteins have been identified so far. The most important and well-studied selenoproteins is glutathione peroxidase (GPx). It is an antioxidant enzyme that detoxifies peroxides, by converting them to either water or less reactive species.

Compared to its lighter analogue sulfur, selenium is much less abundant in cells^{7,8}. Although the general properties such as ionic radii, electronegativity of sulfur and selenium are similar, they show difference in polarizability (2.9 \AA^3 for sulfur, 3.8 \AA^3 for selenium). The widely varying pKa values of $\text{H}_2\text{NCH}(\text{COOH})\text{CH}_2\text{-EH}$ ($\text{E} = \text{S}$ or Se ; 8.3 for SH and 5.2 for SeH), make selenocysteine much stronger nucleophile and better reductant than cysteine at physiological pH⁸. These differences enhance the redox reaction rates of selenium compounds with reactive oxygen species. All these advantages of selenium over sulfur prompted researchers to speculate that selenium compounds may be explored as new class of antioxidants and radioprotectors.

Interestingly the thyroid gland, which is radioresistant, has high selenium contents and about eleven selenoproteins are expressed in the gland.

A few selenium compounds in both inorganic and organic forms have been evaluated for radioprotection⁴. Sodium selenite was the first selenium compound tested for radioprotection in mice. When administered intraperitoneally (i.p.) before (-24 h and -1 h) or shortly (+ 15 min) after irradiation, it increased the 30-day survival of mice irradiated at 9 Gy (DMF = 1.1). Further, its injection 24 hours before amifostine treatment decreased the lethal toxicity and enhanced the radioprotective effect of amifostine significantly. Selenite was also effective when administered in combination with vitamin E before γ -irradiation and prevented the radiation-induced reduction in levels of antioxidant enzymes⁴. It showed a significant protective effect during the initial treatment phase of fractionated therapy. Recent scientific research has also indicated that selenite exhibits differential radioprotection. Based on all these studies, selenite was even tested in clinic at a dosage of $500 \mu\text{g}$ per day, where it reduced the side effects of radio-chemotherapy in head and neck cancer patients⁹.

A few organoselenium compounds like selenourea, selenocystine, selenoxanthene, and



Scheme 2: Selenium compounds examined for radioprotection

selenomethionine, have also been examined for radioprotection using *in vitro* and *in vivo* models^{4,10}. However, these agents did not show much promising activity, except selenomethionine, which has significantly increased the 30-day survival of mice irradiated at lethal doses of radiation. It was equally protective when administered at 24 h, 1 h and 15 min prior to γ -irradiation⁴. However, when selenomethionine was provided in the diet as selenous yeast it showed no protection against acute or chronic radiation exposure. Both selenite and selenomethionine showed remarkable chemopreventive activities in human clinical trials, the former exhibiting far better activity. Very recently, a

synthetic organoselenium compound ebselen, a well-studied GPx mimic, has also been tested for radioprotection in mice. The results indicated that ebselen administration for 14 days at a daily dosage of 10 mg/kg body weight before whole body irradiation at 8 Gy provided substantial protection (60%) against mortality and oxidative damage¹¹. The results reported from various labs support the argument that selenium compounds have great potential to be developed as radioprotectors. Since selenium in organic form exhibits lower toxicity than in inorganic form, extensive research on modulation of radiation-induced changes by new organoselenium compounds is required.

Table 1: Investigations related to the radioprotective efficacy of DSePA

Investigations		Systems monitored	Summary of Results	Reference
GPx-like activity		Enzyme kinetics specificity to hydroperoxide and thiol	Acts as a GPx-mimic with	13
<i>In vitro</i> antioxidant activity		Inhibition of reactive oxygen species induced haemolysis in human RBCs	Inhibits lipid peroxidation of RBC membrane, loss of hemoglobin and K ⁺ ions	15
<i>In vitro</i> radioprotection studies		Protection to biomolecules like DNA, lipids and proteins DNA, peroxidation of lipids and oxidation of proteins	Inhibits radiation induced strand break formation in	14
Acute toxicity studies		Swiss albino mice; Mode of injection: intraperitoneal (i.p.)	Maximum tolerated dose = 8.86 mg/kg	17
In vivo radioprotection studies DSePA dosage: 2mg/kg body weight, i.p. five days prior to irradiation	Hepato (liver) protection	Modulation of antioxidant levels and oxidative stress (5 Gy)	Prevents oxidative stress and depletion of antioxidant enzymes and restored the normal hepatic function and architecture	17
	Hematopoietic protection (5 to 7 Gy)	1) DNA damage in leukocytes 2) Spleen parameters and cell death	Inhibits DNA damage in blood leukocytes, and improved spleen index	17
	Gastrointestinal (GI) protection (7 Gy)	Oxidative stress in small intestine and death of epithelial cells	Reduced oxidative stress and prevented morphological changes and apoptosis in intestinal tissue	18
	Survival studies (9 Gy)	30 days survival	Improved survival of mice by 35%	17
	Immuno-modulation (7 Gy)	1) Intestinal inflammation 2) Cytokines in serum	Ameliorated intestinal inflammatory response and restored immune balance.	18

Radioprotection studies on organoselenium compounds from our laboratory

Our group has initiated a project on development of low molecular weight water-soluble organoselenium compounds as radioprotectors. A number of organoselenium compounds new as well as previously reported were synthesized in our laboratory¹². To enhance the water solubility, functional groups like -OH, -NH₂, -COOH were incorporated in these molecules.

Further, the compounds were examined for free radical reactions, GPx mimicking ability and antioxidant activity. In vitro studies performed on all these compounds indicated that organic diselenides substituted with carboxylic acid functional group are very effective as antioxidants due to less toxicity, ability to scavenge oxidizing free radicals and preventing membrane peroxidation¹³⁻¹⁵. Therefore, diselenodipropionic acid (DSePA), a diselenide, was selected for *in vitro* and *in vivo* radioprotection studies (Table 1). DSePA participates in electron transfer reactions, and the active intermediates produced in the redox reactions can get incorporated in to the GPx enzyme catalytic cycle

of DSePA. It scavenges reactive oxygen species very efficiently and in vitro studies confirmed its potential antioxidant and radioprotecting ability¹³⁻¹⁶.

The maximum tolerable dose (MTD) of DSePA in mice was found to be 8.82 mg/kg body weight¹⁷. Therefore, for *in vivo* radioprotection studies, a non-toxic dose of 2mg/kg body weight, of DSePA was injected intraperitoneally (i.p.) in mice for five days and one hour after the last dose, the mice were exposed to whole body γ -radiation of ~ 9 Gy. Their survival was monitored for 30 days daily and compared with that of radiation and DSePA control animals. There was a significant 35% improvement in the survival of animals treated with DSePA and exposed to radiation as compared to radiation control animals¹⁷. No death was observed in animals treated with DSePA alone. From this study, the dose modification factor (DMF) was estimated to be 1.1. Further DSePA showed significant protection to radiosensitive organs like gastrointestinal (GI) tract, and hematopoietic system, as shown in Figure.1^{17,18}. In the irradiated mice, DSePA maintained the villi height and villi/circumference of the small intestine and prevented epithelial cells (intestinal lining) from undergoing apoptosis. DSePA also exhibited prophylactic action in the hepatic system of

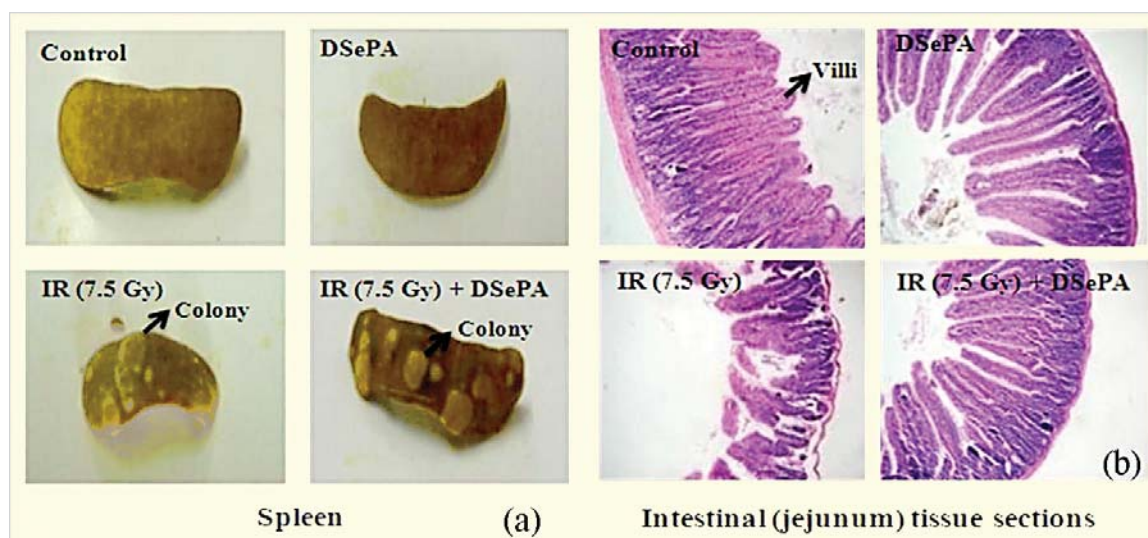


Fig. 1: Pretreatment with DSePA (i.p.) at a dosage of 2 mg/kg body weight protected hematopoietic system and gastrointestinal system as shown by spleen colony formation (A) and maintenance of villi height and numb circumference (b) respectively

irradiated mice through maintenance of the antioxidant enzymes (e.g. GPx) and hepatic architecture. Similarly, DSePA prevented DNA damage in peripheral leukocytes in mice exposed to radiation. Additionally DSePA ameliorated the radiation-induced inflammation and restored the immune balance in irradiated mice.

In conclusion, our *in vitro* and *in vivo* studies on organoselenium compounds revealed that DSePA, a low-molecular weight water-soluble compound with a very low cytotoxicity, is a promising candidate as a radioprotector. Therefore, our future studies are directed to test this compound for tumor selectivity in irradiated animals followed by different phases of preclinical and clinical evaluation. Further, efforts will also be made to design new synthetic derivatives with improved radioprotecting ability.

Acknowledgements

The authors are grateful to Dr. T. Mukherjee, Director Chemistry Group, Dr K. B. Sainis, Director, Bio-Medical Group, Dr S. K. Sarkar Head, RPC Division and Dr. D. Das, Head, Chemistry Division for constant encouragement and support to this work. We are thankful to Board of Research in Nuclear Sciences (BRNS) for the research grant under the Prospective Research Fund (PRF) Scheme (Grant No. BRNS/2007/38/5). We sincerely thank our collaborators and research students, for their enthusiasm and dedication in the execution of the programme.

References

1. Riley, P. A. Free radicals in biology: oxidative stress and the effects of ionizing radiation. *Int J Radiat Biol* 65 (1994): 27-33.
2. Sonntag, C. V. The chemical basis of radiation biology. Taylor & Francis, London, 1987.
3. Carr, K. E., Hume, S. P., Ettarh, R. R., Carr, E. A., McCollough, J. S. Radiation-induced changes to epithelial and non-epithelial tissue. In: Dubois, A., King, G. L., Livengood, D. R. (ed) Radiation and the Gastrointestinal Tract, CRC Press, Boca Raton, 1995.
4. Weiss, J. F., Landauer, M. R. Protection against ionizing radiation by antioxidant nutrients and phytochemicals. *Toxicology* 189 (2003): 1-20.
5. Andreassen, C. N., Grau, C., Lindegaard, J. C. Chemical radioprotection: a critical review of amifostine as a cytoprotector in radiotherapy. *Semin Radiat Oncol* 13 (2008): 62-72.
6. Burdelya, L. G., Krivokrysenko, V. I., Tallant, T. C., Storm, E., Gleiberman, A. S., Gupta, D., Kurnasov, O. V., Fort, F. L., Osterman, A. L., DiDonato, J. A., Feinstein, E., Gudkov, A. V. An agonist of toll-like receptor 5 has radioprotective activity in mouse and primate models. *Science* 320 (2008): 226-230.
7. Papp, L. V., Lu, J., Holmgren, A., Khanna, K. K. From selenium to selenoproteins: synthesis, identity, and their role in human health. *Antiox Redox Signal* 9 (2007): 775-806.
8. Wessjohann, L. A., Schneider, A., Abbas M., Brandt, W. Selenium in chemistry and biochemistry in comparison to sulfur. *Biol Chem* 388 (2007): 97-1006.
9. Buntzel, J., Micke, O., Kisters, K., Bruns, F., Glatzel, M., Schonekaes, K., Kundt, G., Schafer, U., Mucke, R. Selenium substitution during radiotherapy of solid tumors – laboratory data from two observation studies in gynecological and head neck cancer patients. *Anticancer Research* 22 (2005): 211-215.
10. Micke, O., Schomburg, L., Buentzel, J., Kisters, K., Muecke, R. Selenium in Oncology: From Chemistry to Clinics. *Molecules* 14 (2009): 3975-3988.
11. Tak, J. K., Park, J. W. The use of ebselen for radioprotection in cultured cells and mice. *Free Radic Biol Med* 46 (2009): 1177-1185.

12. Jain, V.K., Priyadarsini, K.I. Organochalcogen compounds in material science and biology-a review. *Proc Nat Acad Sci India*, 80 (2010): 269-280.
13. Mishra, B., Barik, A., Kunwar, A., Kumbhare, L. B., Priyadarsini, K. I., Jain, V. K. Correlating the GPx activity of selenocystine derivatives with one-electron redox reactions. *Phosphorus, Sulfur, Silicon and Related Elements* 183 (2008): 1018–1025.
14. Santoshkumar, B., Kunwar, A., Ahmad, A., Kumbhare, L. B., Jain, V. K., Priyadarsini, K. I. In vitro radioprotection studies of organoselenium compounds: differences between mono- and diselenides. *Radiat Environ Biophys* 48 (2009): 379–384.
15. Kunwar, A., Mishra, B., Barik, A., Kumbhare, L. B., Pandey, R., Jain, V. K., Priyadarsini, K. I. 3, 3'-Diselenodipropionic acid, an efficient peroxy radical scavenger and a GPx mimic, protects erythrocytes from AAPH induced haemolysis. *Chem Res Toxicol* 20 (2007): 1482-1487.
16. Mishra, B., Kumbhare, L. B., Jain, V. K., Priyadarsini, K. I. Pulse radiolysis studies on reactions of hydroxyl radicals with selenocystine derivatives. *J Phys Chem B* 112 (2008): 4441-4446.
17. Kunwar, A., Bansal, P., Jaya Kumar, S., Bag, P. P., Paul, P., Reddy, N. D., Kumbhare, L. B., Jain, V. K., Chaubay, R. C., Unnikrishnan, M. K., Priyadarsini K. I. In vivo radioprotection studies of 3,3'-Diselenodipropionic acid (DSePA), a selenocystine derivative. *Free Radic Biol Med* 48 (2010): 399-410.
18. Kunwar, A., Bag, P. P., Chatopadhyay, S., Jain, V. K., Priyadarsini K. I. Anti-apoptotic, anti-inflammatory and immunomodulatory activities of 3,3'-diselenodipropionic acid in mice exposed to whole body α -radiation. *Arch Toxicol* (2011) (in press).

Flow Simulations of Industrial Scale Agitated Tanks

K.K. Singh, K.T. Shenoy and Hanmanth Rao

Chemical Engineering Division

and

S.K. Ghosh

Chemical Engineering Group

Abstract

Single phase flow simulations of two different industrial scale agitated tanks being used at Nuclear Fuel Complex, Hyderabad have been carried out. While one tank is smaller and has a conical bottom, the other tank is bigger and has a dished bottom. The objective of the simulations is to examine and understand the flow patterns in the tanks and to qualitatively decide whether the observed flow patterns are good for suspending solids. The tank with conical bottom is found to have satisfactory flow pattern owing to very low off bottom clearance of the impeller. The tank with the dished end is found to have a flow pattern that may not give adequate solid suspension. Possible changes in the operating parameters and geometry of this tank are evaluated with an objective of improving the flow pattern in the tank.

Introduction

Knowledge based design of solvent extraction equipment is one of the major research areas in Chemical Engineering Division, BARC. Extensive studies, both experimental and computational, have been carried out on solvent extraction equipment¹⁻⁵. The expertise generated in these studies is being applied to develop fundamental understanding of various process equipments being used in DAE. The work reported here is the outcome of one of such studies. Flow simulations can provide useful insight into the working of process equipment eventually leading to their optimum design. In Chemical Engineering Division of BARC, flow simulations studies have been carried out for various process equipments such as pump-mix mixers and leaching reactors. The tanks studied here are used for semi batch precipitation reaction between two liquids – uranyl nitrate pure solution (UNPS) and ammonium hydroxide - resulting in precipitation of ammonium diuranate (ADU) in the form of fine particles. Ammonium hydroxide is dripped gradually

from the top of the tank while agitation is on. Over the batch time liquid level in the tank rises. The precipitated particles are to be kept under suspension. At the end of the operation, slurry is routed to a filter while keeping the agitator on.

Flow simulations of existing tanks

Geometry

The important dimensions of both the tanks are given in Table 1. The final level given in Table 1 is the level at the end of the batch.

Table 1: Important dimensions of smaller and larger tanks

	Smaller Tank	Larger Tank
Tank diameter (mm)	1900	2300
Impeller diameter (mm)	1150	1460
Liquid level from bottom (mm)	2150	2710
Impeller off bottom clearance	255	438

There are three impellers in both the tanks. Each impeller consists of two blades. Each blade has got two parts – inner blade which is down-pumping and outer blade which is up-pumping. The tanks also have helically arranged steam coils. Geometries which have been used in simulations are shown in Fig.1. Helical coils have been approximated as circular coils to make geometry simpler.

Flow patterns

Single phase flow simulations were carried out for designed operating speed of the tanks (48 rpm for the larger tank and 56 rpm for smaller tank). The fluid assumed in the simulation is the filtrate obtained after filtration having density and viscosity equal to 1022 kg/m³ and 0.77 cP, respectively. The top surface is the air-liquid interface and has been modeled as a

wall with zero shear stress. Fig. 2 shows the vector plot in a vertical central plane for smaller tank. The downward flow in the centre of the tank can be attributed to the inner down-pumping blades. Surrounding this downward flow is upward flow attributed to the up-pumping by outer blades. There is an interaction between the inner blades and outer blades as part of the downward flow from inner blades is picked up by the outer blades. Similar flow pattern is observed for the bigger tank as shown in Fig. 3. The mass flow rates at various planes in both smaller and larger tanks are shown in Fig. 4 with

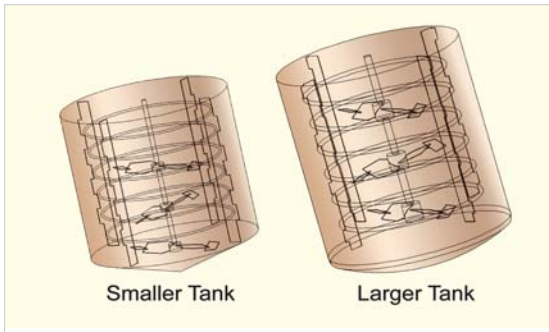


Fig. 1: Geometries of the smaller tank and the larger tank used for simulations

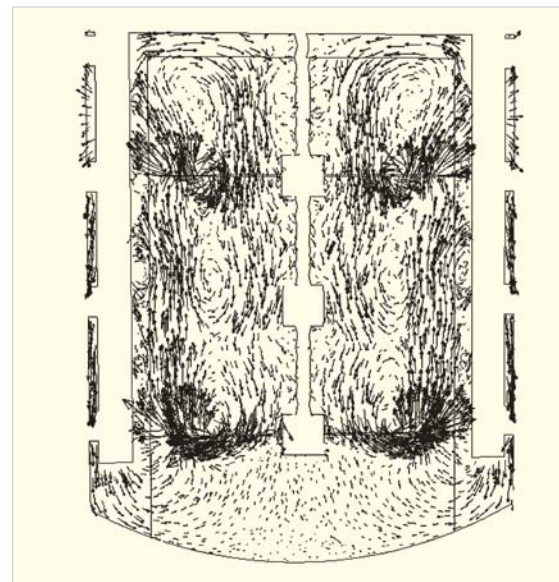


Fig. 3: Flow pattern in the larger tank

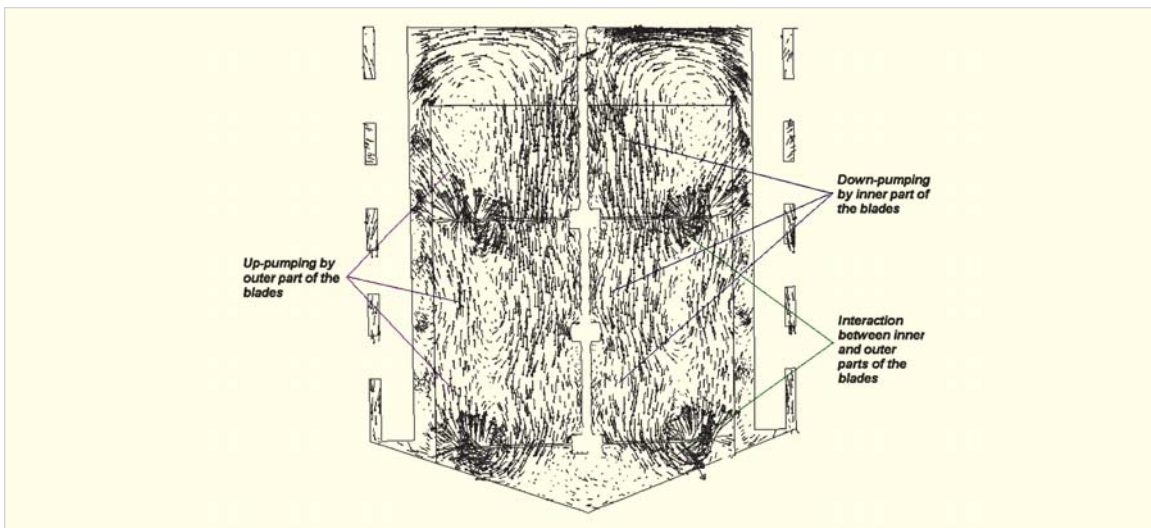


Fig. 2: Flow pattern in the smaller tank

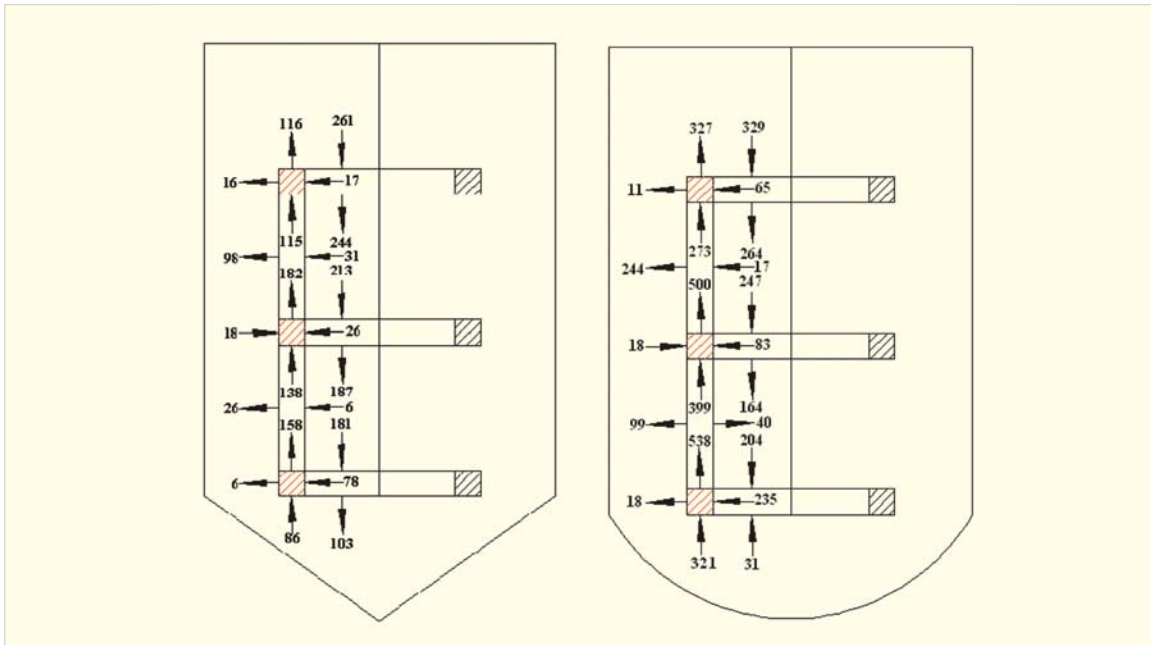


Fig. 4: Mass flow rates at different planes in the smaller and larger tank

Table 2: Power inputs, specific power input and power number of agitator in smaller tank

Impeller inner blades	Power input by outer blades	Power input by both the blades	Power input by
Upper	34	173	208
Middle	55	156	211
Lower	99	208	307
Total power input		726	
Specific power input		145	
Power number		0.43	

Table 3: Power inputs, specific power input and power number of agitator in larger tank

Impeller	Power input by inner blades	Power input by outer blades	Power input by both the blades
Upper	65	452	517
Middle	141	424	565
Lower	342	523	865
Total power input		1946	
Specific power input		175	
Power number		0.56	

impeller swept volumes shown as rectangular blocks. Outer blades are shown as red-thatched blocks. As can be seen for smaller tank there is net downward flow in the inner core due to down-pumping inner blades and there is net upward flow in the outer core due to up-pumping outer blades. The most important finding of the simulations is that there is an interaction between the inner and outer blades due to which the downward flow is depleted as it moves from top to bottom. Due to interaction between the inner and outer blades the inner core of downward flow is depleted from 261 to 106 kg/s in the smaller tank. The interaction between the outer blades and the inner blades is stronger in case of larger tank and the downward flow in the inner core is completely sucked by the outer blades and the flow at the bottom of the tank becomes upward instead of being downward. According to Bakker⁶, Murthy⁷ downward flow is more efficient than upward flow for solid suspension. The upward flow at the bottom of the larger tank is, therefore, not desirable and should be avoided.

Power input values

From the flow field resulting from simulations the power consumed by different blades have been obtained and compiled in Table 2 and Table 3. Power values are in W and specific power input is in W/m³. Power number is based on power consumed by all the three impellers.

Despite of smaller blade area compared to the inner blades, power input by the outer blades is more than that by the inner blades. This is attributed to the higher torque by the outer blades due to their longer radial distances from the shaft. The power input by the lower impeller is the highest, followed by the middle impeller and top impeller. The power input by the upper impeller is marginally smaller than that by the middle impeller. Power input by the inner blades is the highest for the lower impeller followed by the middle impeller and then the upper impeller. Power input by the outer blades is the

highest for the lower impeller and lowest for the middle impeller. These apply to both the tanks. The specific power input for larger tank is about 20% higher than that of the smaller tank. The power number of agitator of the larger tanks is about 30% more than that of the smaller tank.

Evaluation of various options to modify flow pattern in larger tank

Increase in impeller speed

Among different options evaluated to improve the flow pattern in the larger tank, first one was to increase impeller speed. Simulation was carried out for 56 rpm instead of 48 rpm. The flow pattern and mass flow rates obtained from flow simulations are given in Fig.5. On comparing the mass flow rates in Fig. 5 with that of mass flow rates for larger tank in Fig.4, it is seen that flow pattern remains the same. Increasing impeller speed has only enhanced the flow rates while the flow at the bottom of the tank with increased impeller speed is still upward. Increase of impeller speed, therefore, cannot be an option to ensure proper flow pattern.

Reduction in clearance

A round of simulation was carried out for the geometry in which impeller assembly of the larger tank was brought down by 278 mm such that the lower impeller is in the plane at which the dished end and the cylindrical surface of the tank join. The result of this simulation is shown in Fig. 6. As can be seen, flow at the bottom of the tank become downward but the magnitude is not much. Another round of simulation was carried out by bringing the impeller assembly further down by 210 mm. The downward flow at the bottom of the tank was found to increase from 95 kg/s to 175 kg/s. Therefore, lowering the impeller assembly is one of the options to ensure proper flow pattern in the larger tank.

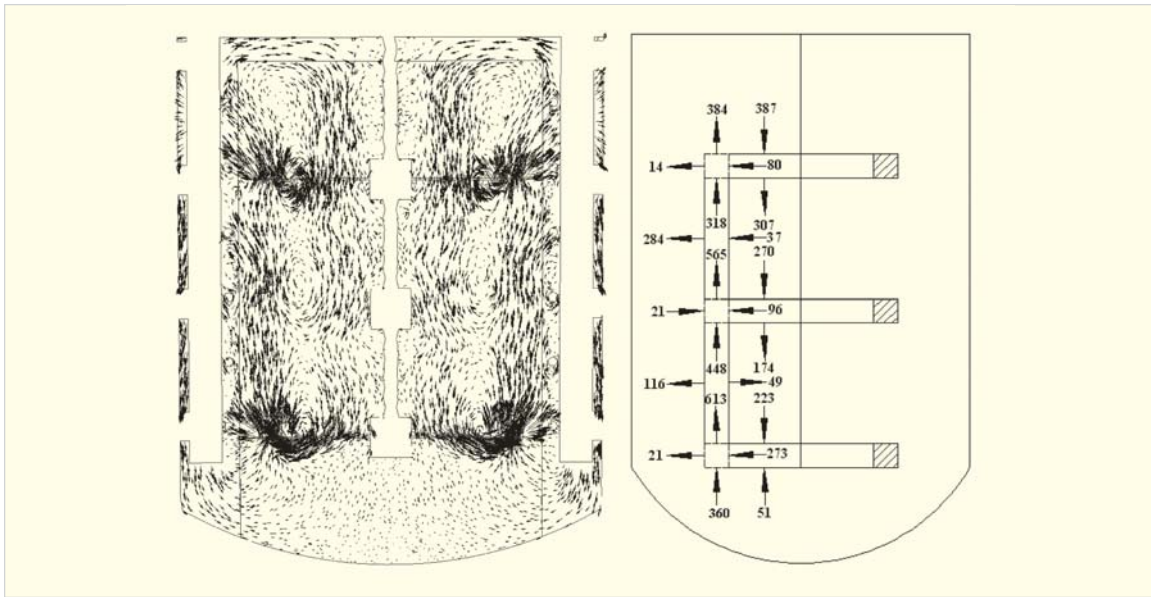


Fig. 5: Flow pattern and mass flow rates at different planes for larger tank at 56 rpm

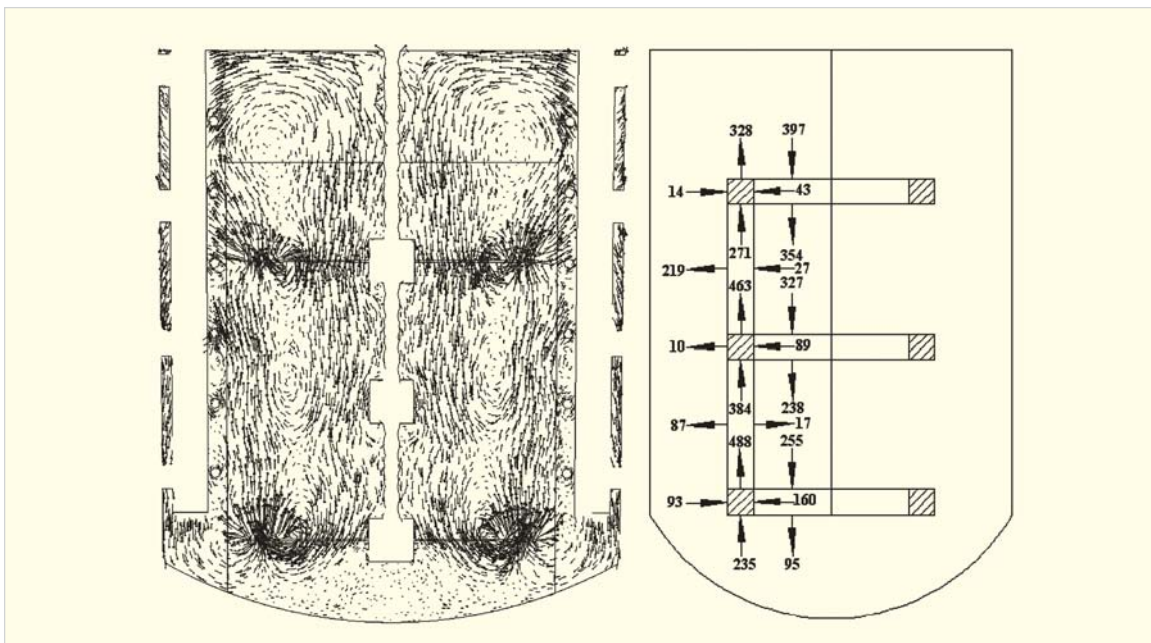


Fig. 6: Flow patterns and mass flow rates at different planes for larger tank with reduced impeller clearance

Modification in the lower impeller

Another round of simulation was carried out with the geometry in which the outer blades of the lower impeller were removed. Results of the simulation for this modified geometry are shown in Fig. 7. The downward flow at the bottom is now 295 kg/s. But in this case the flow exchange between the lower

impeller and the inner blades of the middle impeller is not much. There appears to be a local recirculation loop formed around the lower impeller. According to Coker⁸ this kind of zone mixing should be avoided in multiple impeller system. Solid suspension in the bottom portion of the tank may be better but may not be very uniform for the entire height of the tank.

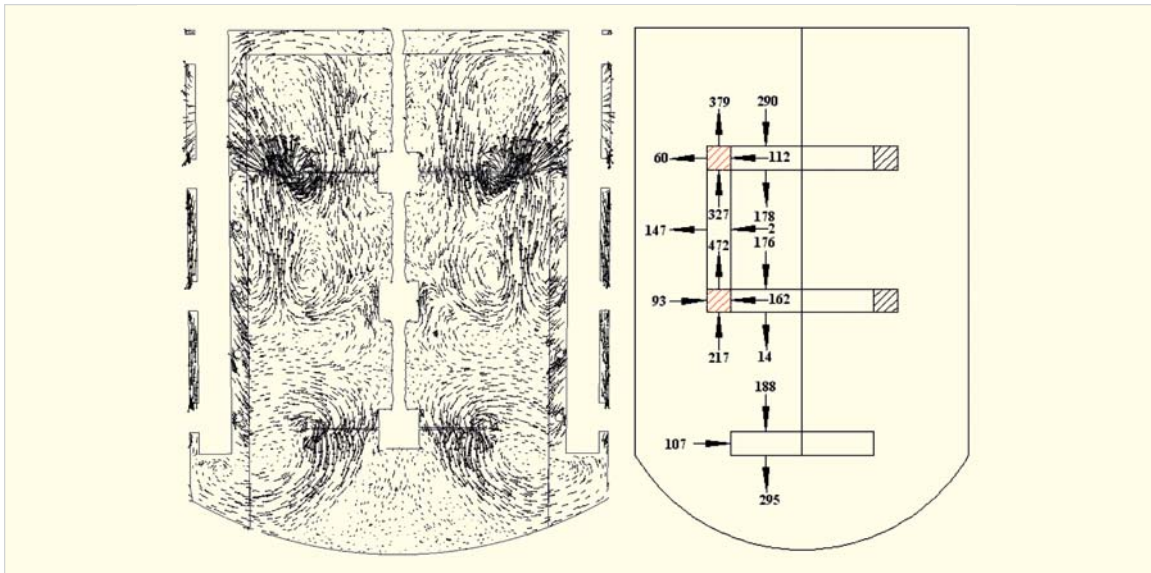


Fig. 7: Flow patterns and mass flow rates at different planes for larger tank with modification in lower impeller

Modification in all the impellers

In the fourth option evaluated here, outer blades of all the impellers were removed. Results of the simulation for this modified geometry are shown in Fig. 8 which shows that if outer blades of all the impellers are removed, the flow pattern becomes

similar to classical flow pattern of a pitched blade turbine - downward flow in the centre and upward flow along the walls of the tank. The discharge from the lower impeller is more than the suction flow rate of the upper impeller and is very high - highest of all the options evaluated so far. Taking out the outer blades of all impeller thus appears to be a

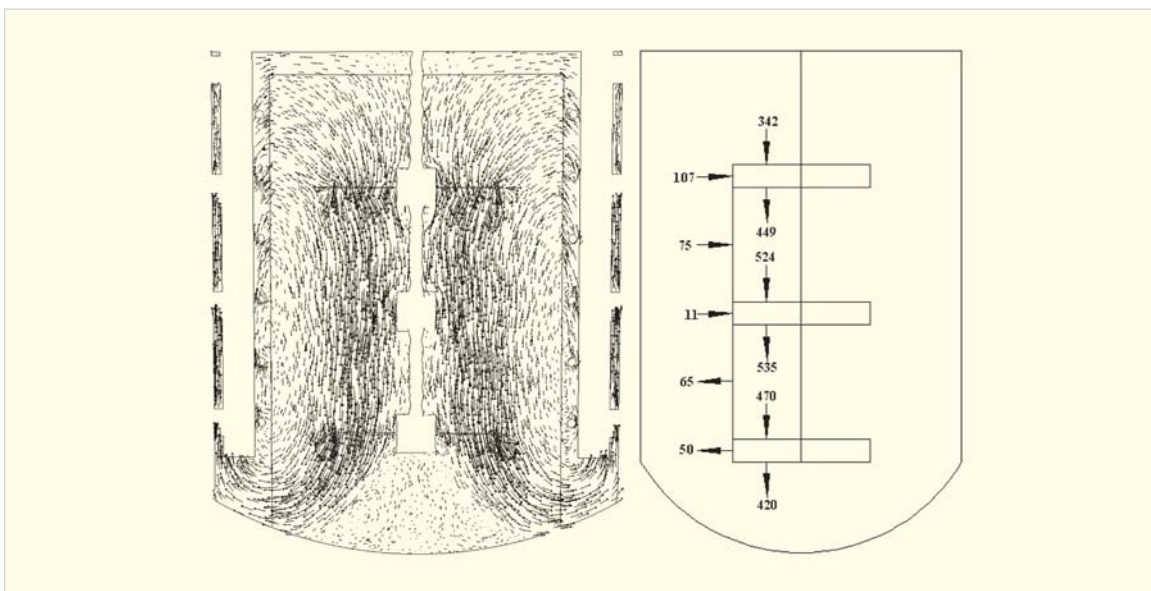


Fig. 8: Flow patterns and mass flow rates at different planes for larger tank with modification in all the impellers

good option to ensure good solid suspension. There is a volume of the tank below the hub of the lower impeller wherein the velocities are not high. This volume can be reduced by changing the blade angle which in the present design is 30° and clearance of the impeller. Probably taking out the outer blades of all the impellers and simultaneously bringing down the impeller assembly will be the best option to improve the flow pattern to ensure adequate solid suspension.

Simulation of smaller tank with up-lifted impeller assembly

One more simulation was carried out to see what happens if the impeller assembly is lifted up in the smaller tank. Fig.9 shows the results of this simulation in which the impeller assembly has been raised by 250 mm. As can be seen, for this geometry also the flow at the bottom becomes upward. It is, therefore, concluded that the flow pattern in the bottom of the tank is a strong function of impeller off-bottom clearance.

Conclusions

Flow patterns in two designs of ADU precipitation tanks are compared using single phase flow simulations. Flow simulations clearly bring out that there is strong interaction in the outer and inner blades of the impellers being used in the tanks. Impeller off-bottom clearance also has a strong influence on the flow pattern in the bottom of the tanks. The flow patterns in the larger tank are found to be undesirable for suspending solids. This is attributed to interaction between the outer up pumping blades and inner down pumping blades of the impellers. Various options to improve the flow pattern in the larger tank are evaluated using flow simulations. Results of the simulations reveal that very high downward flow in the bottom of the tank can be obtained by taking out the outer blades of the impellers ensuring better solid suspension.

Acknowledgements

The authors gratefully acknowledge NFC Hyderabad for the inputs for this work and Department of Chemical Engineering, IIT Bombay for allowing use of computational resources.

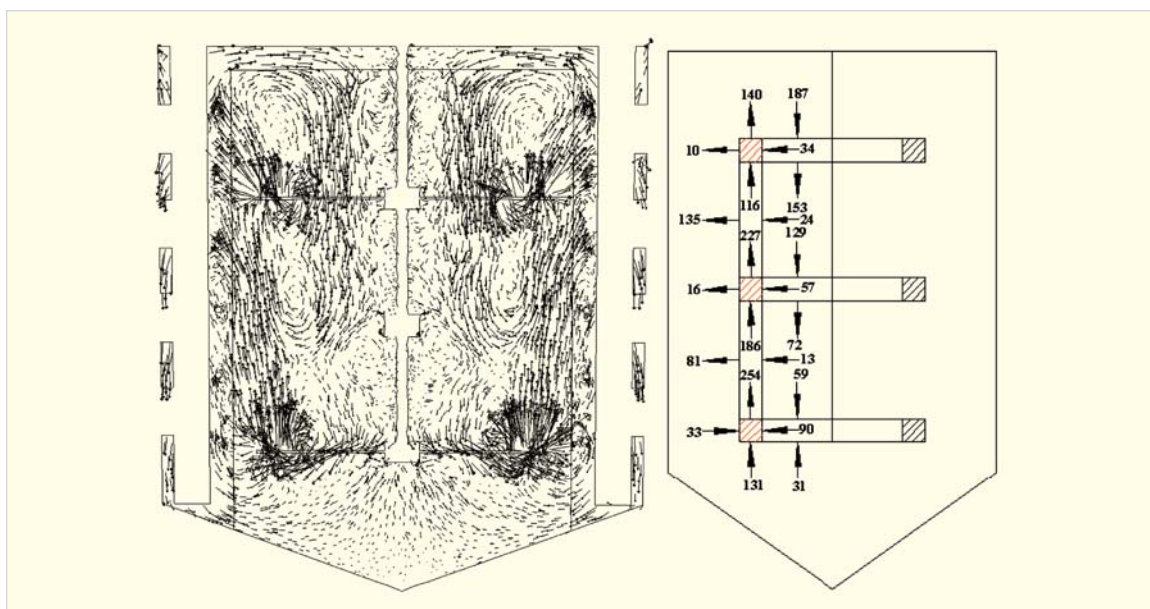


Fig. 9: Flow patterns and mass flow rates at different planes for smaller tank with impeller assembly lifted up

References

- 1 Singh K.K., Shenoy K.T., Mahendra A.K., Ghosh S.K. "Artificial neural network based modeling of head and power characteristics of pump-mixer". *Chemical Engineering Science* 59 (2004): 2937-2945.
- 2 Singh K.K., Mahajani S.M., Shenoy K.T., Patwardhan A.W., Ghosh S.K. "CFD modeling of pilot-scale pump-mixer: Single-phase head and power characteristics". *Chemical Engineering Science* 62 (2007): 1308-1322.
- 3 Singh K.K., Mahajani S.M., Shenoy K.T., Ghosh S.K. "Computational Fluid Dynamics modeling of a bench-scale pump-mixer: Head, power and residence time distribution". *Industrial Engineering & Chemistry Research* 46 (2007): 2180-2190.
- 4 Singh K.K., Mahajani S.M., Shenoy K.T., Ghosh S.K. "Representative drop sizes and drop size distributions in A/O dispersions in continuous flow stirred tank". *Hydrometallurgy* 90 (2008): 121-136.
- 5 Singh K.K., Mahajani S.M., Shenoy K.T., Ghosh S.K. "Population balance modeling of liquid-liquid dispersions in homogeneous continuous-flow stirred tank". *Industrial Engineering & Chemistry Research* 48 (2009): 8121-8133.
- 6 Bakker A., Fasano J.B., Myers K.J. *Effect of flow pattern on the solids distribution in a stirred tank*. <http://www.bakker.org/cfmbook/solids.pdf> (accessed on March 8th, 2011)
- 7 Murthy B.N., Ghadge R.S., Joshi J.B. "CFD simulations of gas-liquid-solid stirred reactor: Prediction of impeller speed for solid suspension". *Chemical Engineering Science* 63 (2007): 7184-7195.
- 8 Coker A.K. *Ludwig's Applied Process Design for Chemical and Petrochemical Plants, Volume 1, Fourth Edition*. Gulf Professional Publishing, 2007.

Experiments on Reinforced Concrete Structures: Sub-Assemblages and Components for Seismic Safety: Post Installed Anchors

Akanshu Sharma, P.N. Dubey, G.R. Reddy and K.K.Vaze

Reactor Safety Division

and

C. Mahrenholtz and R. Eligehausen

Institut für Werkstoffe im Bauwesen, Universität Stuttgart, Germany

and

C.C. Gupta and J.K. Chakravartty

Mechanical Metallurgy Division

and

S.K. Mishra, S. Guha and R.L. Suthar

Centre for Design and Manufacture

and

T.V.S. Murthy and K. Srinivas

Architecture and Civil Engineering Division

Abstract

Post Installed (PI) mechanical anchors/fasteners such as undercut anchors, expansion anchors etc. are a versatile means of forming connections in concrete structures. They find widespread application for the fastening of structural elements, such as dampers, stiffeners, bracings etc. and equipments and piping systems to concrete structures. The fulfillment of the desired objectives of the structural elements, equipments, and piping is largely dependent on the behavior of fasteners. Especially in the case of nuclear installations, failure of anchorage during a seismic event may lead to devastating damages. For example it may lead to failure of certain important components or equipments or piping. Only limited experimental data at cycling frequencies lower than that encountered during seismic events are available and used for design of anchors. For design and evaluation purposes, it is conservatively assumed that the anchor is installed in a pre-existing crack. Therefore seismic action mainly induces three types of loading namely, cyclic tension, cyclic shear and cyclic opening and closing of cracks. Out of these, the cyclic opening and closing of cracks is one of the most demanding types of excitation for post-installed anchors. In this work, experiments were performed under the framework of Indo-German collaborative programme between Reactor Safety Division (RSD) and Institut für Werkstoffe im Bauwesen, Universität Stuttgart, Germany on post-installed undercut type anchors installed in cracks under crack opening and closing at different frequencies. The purpose of the experiments was to evaluate the effect of the crack cycling frequency on the load displacement behavior. Various divisions of BARC were involved in the project. The specimens were cast at the Common Facility Building (CFB) site by RSD and Architecture and Civil Engineering Division (A&CED), BARC and the experiments were performed at Component Test Facility (CTF) of Mechanical Metallurgy Division (MMD), situated at Centre for Design and Manufacture (CDM), BARC.

Introduction

Anchors or fasteners are frequently used to connect structural and non-structural systems, sub-systems, components, piping, equipments etc. to the concrete structure. The structure which supports equipment, piping systems etc. is called primary structure (PS) and the supported equipments, piping systems etc. are called secondary structure (SS). Primary seismic members or structural elements are the members considered as part of the primary structural system that resists the seismic action and that are modeled for seismic analysis. SS are light with small relative stiffness compared to the PS. In view of this only mass of SS are considered in modeling and analysis of the PS. Fig. 1 (Hoehler, 2006) shows the use of anchors for connecting structural and non-structural systems to the primary structure.

Although, in nuclear industry, the use of cast-in-place anchors also known as embedded parts (EP) is widespread, it is impossible to pre-plan every component along with its location at the design stage. Therefore, invariably, post-installed anchors are often used for fixing the SS to PS. The safety of the SS connected to the PS with the anchors is highly dependent on the performance of the anchor itself. In turn, the safety of the anchors is dependent on the proper design of the anchors and suitability of the anchor for the said application. The design of post-installed anchors has developed over the years and is now well-documented in text (e.g. Eligehausen et al, 2006), technical specifications (e.g. CEN TC/250) and in standards (e.g. ACI 318, 2008). However, the available documents mainly address the issue of design under static loads and not much is said about the suitability and design of the anchors for seismic applications. It is generally assumed, judiciously conservatively, that an anchor is installed in a crack, pre-existing or formed during earthquake. Therefore, during an earthquake, an anchor may be subjected to cyclic tension, cyclic shear and cyclic opening and closing of the crack.

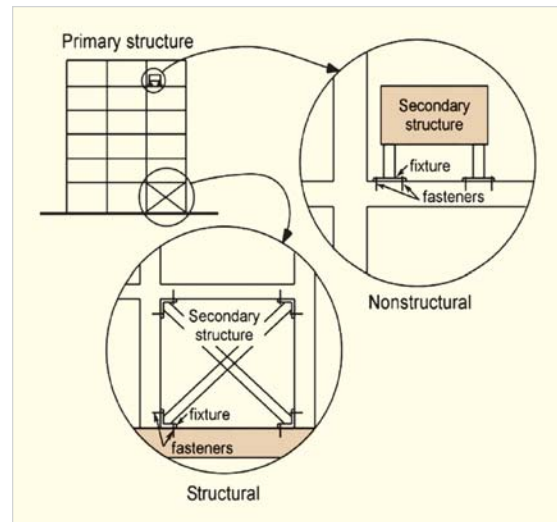


Fig. 1: Structural and Non-Structural Applications of Fastenings (Hoehler, 2006)

The tension performance of anchors located in cracks can be significantly affected by the number of crack cycles, the load applied and the ratio of minimum to maximum crack width during cycling (Eligehausen et al, 2006).

The anchors used in concrete structures may be classified broadly as cast in place anchors and post-installed anchors. The cast-in-place anchors are embedded in the concrete and are in form of threaded sleeves, channel bars, headed studs etc. The post-installed anchors are installed in the concrete after hardening mostly by drilling a hole. Expansion anchors, undercut anchors, bonded anchors, bonded-expansion anchors, bonded-undercut anchors, screw anchors etc. are few of post-installed anchors.

Anchors transfer the applied tension loads to concrete in any one or combination of following three mechanisms, namely: Mechanical interlock; Friction; and Bond. Mechanical interlock refers to the mechanism where load is transferred by means of a bearing interlock between the anchor and concrete. Headed anchors, anchor channels, screw anchors and undercut anchors employ this mechanism. Friction is the load transfer mechanism

load cell, high capacity 2 stage servo valve attached to a pre-loaded swivel base and swivel rod end for both static and dynamic test applications. The actuators are shown in Fig. 4 (a). The actuators are operated by windows based control system software with programming facilities to impart both pre-programmed and custom profiles for facilitating static and dynamic tests on components under load, displacement or strain control modes. The controller unit remotely powers the HPS and the actuators to work on the three control modes. The control room housing the controller and software is shown in figure 4 (b). The hydraulic system is powered by large HPS (~800 Lit capacity) delivering oil at 3000 psi or 20.7 bar to the actuators.

In addition, the control of the actuators using external analog signals as well as a computed signal using different functions based on real analog signal inputs is also possible. This feature has been used in the anchor response tests, utilizing signals from a fatigue rated HBM make LVDT (10 mm stroke and resolution of 1 μ m) to control the actuator. Special programming to facilitate multiple (in this case two) analog inputs were implemented to achieve control of two actuators simultaneously based on the variation of the computed mean. The opening or closing of the LVDT indicated the extent of change in the crack width, which determined the loading sequence to initiate dynamic cycles on the anchor embedded in the pre-cracked concrete.

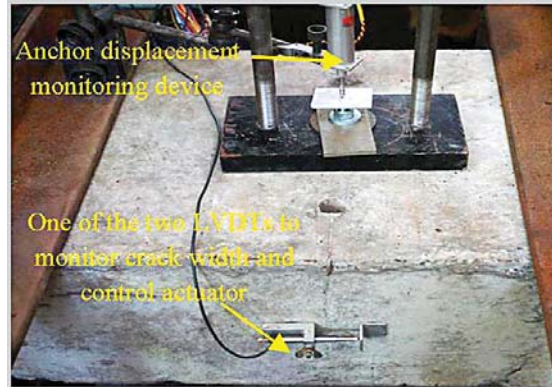


Fig. 5: Crack Width and Anchor Displacement Measuring Devices

In the present tests the signals from the two LVDT were first combined to compute the mean, thereby representing mean crack width opening for controlling the loading sequence. During the tests load, actuator displacement, crack width (both from the individual LVDT and the mean), and anchor displacement were recorded. Fig. 5 shows the LVDT arrangement provided to monitor crack width and the anchor displacement.

Fig. 6 shows a typical test record of the load, crack width and anchor displacement profiles from the test demonstrated to confirm the successful implementation of the program. In the demonstration the concrete specimen was loaded by single actuator as per the profile programmed to open the crack width between 0.25 to 0.45 mm, and cycled at 1 Hz. The data was obtained in a multi-column ASCII format for further analysis.



(a) Actuator System at CTF

(b) Control Programming

Fig. 4: Component Test Facility, MMD, BARC

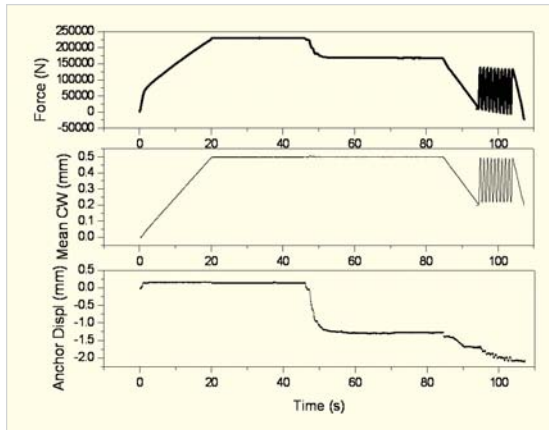


Fig. 6: Typical Test Record

Experimental Setup

The experiment needed to have a setup where a constant tension load is applied on the anchor and then the crack can be opened and closed (cycled) by hydraulic actuator. The fixtures were designed, fabricated and the test setup was prepared by CDM and RSD. Fig. 7 shows the complete setup of the experiment.

Anchor Installation

Under this programme, a self undercutting through-fix anchor (Hilti make) was tested (Fig. 8(a)). The anchor is composed of a formed steel bolt with a conical end, a strong sleeve with a cutting edge which will form the undercut and provide the key effect by deforming, a washer and a nut. It was

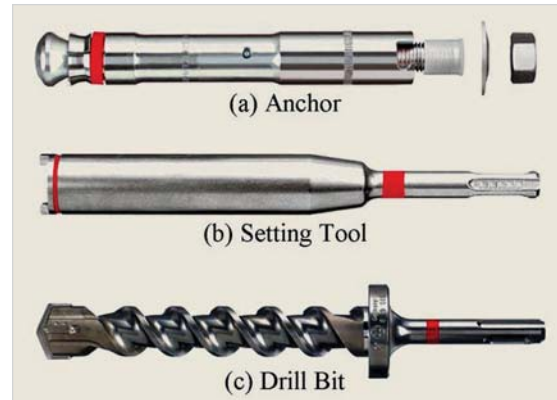


Fig. 8: Anchor and Required Installation Tools (Source: Hilti)

installed with an effective embedment depth, $h_{ef} = 125$ mm. The anchor was installed using setting tool (Fig 8(b)) by turning and hammering in a hole drilled with drill bit (Fig 8(c)), a 4-cutter drill with a stop flange to ensure the correct drill hole depth of 135 mm.

Fig. 9 shows the installation procedure of the anchor in the concrete specimen. First, the hole is drilled at the designated position (Fig. 9 (a)). Then, by hammering the split wedges and sleeves, the crack is induced in the specimen (Fig. 9 (b)). The crack invariably passes through the pre-drilled anchor hole. The split wedges are then removed leaving the hairline crack and the anchor is placed in the hole and installed using the setting tool (Fig. 9 (c)). Generally, a turning time of up to 30 seconds is



Fig. 7: Experimental Setup for the Tests at CTF (CDM, BARC)

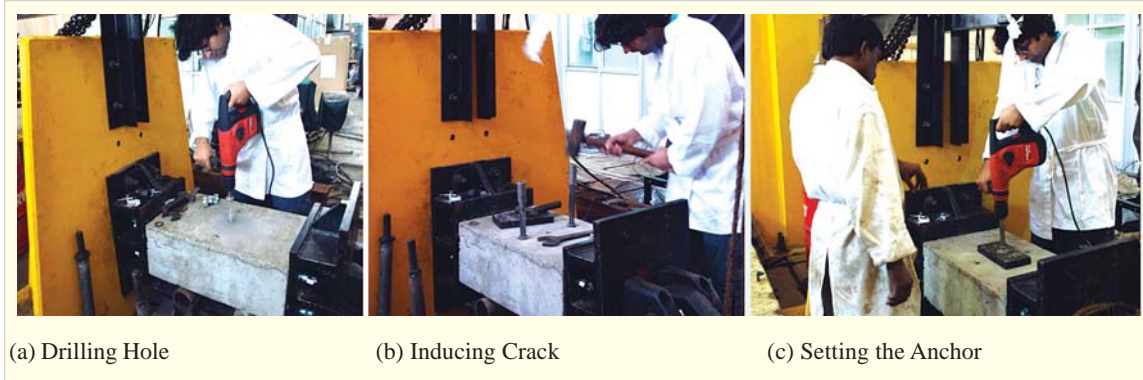


Fig. 9: Installation of Anchor in the Specimen

appropriate for proper setting of the anchor. After setting, the nut is tightened to a torque of 80 N-m which, after about 10 minutes is released to 40 N-m to simulate relaxation in long run.

Loading Pattern

The loading pattern consisted of following steps:

1. Loading the anchor to a specified load (in this case 23.5 kN).
2. Opening the crack to 0.8mm crack width.
3. Closing the crack to 0.5mm crack width.
4. Apply ten cycles of opening and closing of cracks between 0.5mm and 0.8mm at specified frequency (0.005 Hz, 1 Hz, 5 Hz and 10 Hz).
5. Opening the crack to 0.8mm.
6. Pulling out the anchor to obtain residual load.

Typical Experimental Results

Fig. 10 shows the typical results for variation of crack and load v/s time during the crack cycling test and Fig 11 shows the effect of loading rate on the displacement of the anchor. Fig. 10 shows various phases, viz. loading of anchor, crack cycling and pull-out of the anchor. It can be seen that the crack opens when the anchor is being loaded. Thereafter the crack is opened by the actuator to 0.8 mm and then closed to 0.5mm after which the crack is cycled 10 times to simulate seismic shaking. Fig 11 shows that as the loading frequency is increased, the displacement of anchor is reduced.

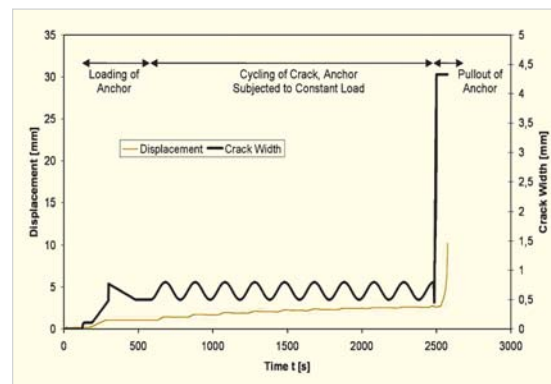


Fig. 10: Variation of crack and anchor load during the test with 0.005 Hz

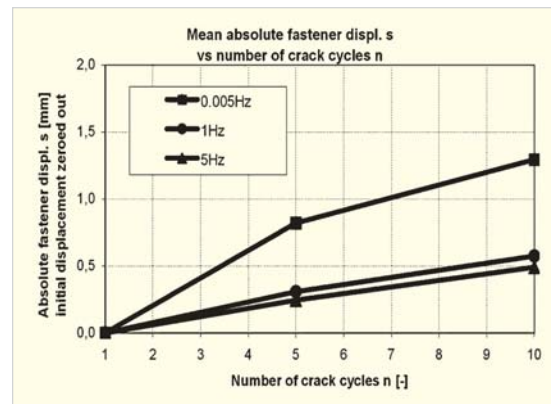


Fig. 11: Displacement of Anchor for various frequencies

Summary and conclusions

Design of post-installed anchors for reinforced concrete structures, in India, is mainly governed by guidelines and suggestions given by the anchor producing companies. Although, international

standards such as ACI, Euro Code, DIN, ETAG etc. and text books such as Eligehausen et al (2006) give guidelines and basis for design of anchors for concrete structures, they are generally not applicable for seismic loading case. In order to bridge this gap and to understand the behaviour of post-installed anchors under earthquakes, experiments were performed on under cut anchors for concrete structures. Experiments were performed under the framework of the Indo-German collaborative project and various divisions of BARC participated in the same. The specimens were cast at the Common Facility Building (CFB) site by Architecture and Civil Engineering Division (A&CED), BARC and the experiments were performed at Component Test Facility (CTF) of Mechanical Metallurgy Division (MMD), Material Group situated at Centre for Design and Manufacture (CDM), BARC. The experiments provided a good insight to the behavior of post-installed anchors under seismic loading and the results of the experimental programme will be useful for generating guidelines for seismic applications of the anchors for fixing systems and components to concrete structures.

Acknowledgements

Many people were involved in the successful completion of the tests. Mr. R.V. Nandanwar, Mr. S.N. Bodele, Mr. M.A. Khan of RSD, BARC; Mr. S.S. Sharma, Mr. Nagare, Mr. Naidu, Mr. M. Nayar of CDM, BARC, Mr Mahadik and Mr. Mujawar of RED, BARC deserve a special recognition for the efforts devoted towards the project. The authors are thankful to Mr. D.G. Belokar, RED for providing manpower support and Megatech Engineering & Services Pvt Ltd, Mumbai for support regarding instrumentation and programming of controls.

References

1. ACI 318:2008, "Building code requirements for structural concrete and commentary" American Concrete Institute, 2008.
2. CEN TC/250, "Design of fastenings for use in concrete-final draft".
3. Eligehausen, R., Mallèe, R., Silva, J.F., "Anchorage in concrete construction", Ernst & Sohn, 2006.
4. Eurocode 8, "Design of structures for earthquake resistance", 2004
5. Hoehler, M.S., "Behavior and testing of fastenings to concrete for use in seismic applications" PhD Dissertation, Institut für Werkstoffe im Bauwesen, Universität Stuttgart, Germany, 2006.

Hollow Fibre Liquid Membranes: A Novel Approach for Nuclear Waste Remediation

S.A. Ansari, P.K. Mohapatra and V.K. Manchanda

Radiochemistry Division

Abstract

Liquid membrane separations using hollow fiber contactors are finding increasing applications in diverse areas including metal ion separations. This technique offers the advantages of active transport, possible usage of exotic carriers, easy scale-up, low energy requirements, low capital & operating costs, etc. At Radiochemistry Division, hollow fiber based separation processes have been developed for actinide partitioning, lanthanide / actinide separation, Sr / Y separation, recovery of radio-caesium and plutonium from various wastes. The physical, chemical and radiolytic stability of the HFSLM system has been investigated. Non-dispersive solvent extraction using hollow fiber contactors has also been employed for the extraction of actinides and lanthanides.

Introduction

Nuclear energy is perceived as a strong candidate for taking care of future energy needs globally particularly due to significantly lower carbon emissions. However, large scale investments in the area are subjective to the development of environmentally safe and robust technologies for the management of High Level Waste (HLW) generated in the back end of the nuclear fuel cycle. The separation processes involved in the back end of the nuclear fuel cycle are predominantly based on solvent extraction. The proposed strategy of 'Actinide Partitioning' for the remediation of HLW is based on solvent extraction of minor actinides using specially designed reagents such as CMPO, diglycolamides and malonamides. Solvent extraction based techniques using exotic reagents such as crown ethers and calix-crowns have also been developed for the recovery of valuable fission products such as Cs-137 and Sr-90 from HLW. In view of the exorbitant cost of some of these extractants as well as the use of large volumes of VOCs, it is imperative to develop separation processes

with much lower inventory of extractants. Liquid membrane (LM) based separations have been reported to be efficient even for large scale metal ion recovery¹. LM based separations are fascinating, as they retain the selectivity features of solvent extraction separations. Out of the LM methods, supported liquid membrane (SLM) appears interesting as the ligand inventories involved are low. There are of course limitations of throughput and stability of the SLM. In this context, SLM based separations using hollow fiber contactors, referred to as Hollow Fibre Supported Liquid Membrane (HFSLM), are particularly attractive due to their large surface to volume ratio, faster mass transfer rates and continuous flow^{2,3}.

Liquid membranes and their classifications

Liquid membranes are broadly classified into three different types, viz. bulk liquid membrane (BLM), emulsion liquid membrane (ELM) and supported liquid membrane (SLM)⁴. BLM is a stirred organic

phase of distinctly different density than the aqueous phase positioned under it or vice versa. In ELM, the receiver aqueous phase containing oil droplets are dispersed into the feed aqueous phase. The volume of the receiving phase inside the oil droplets is at least ten times smaller than that of the source phase. The thickness of the membrane (organic film) is very small, while the surface area is enormous resulting in very fast separation. Though the efficiency of the liquid membrane is inversely proportional to the thickness of the membrane phase, too thin a film has poor stability due to low but finite solubility in feed (source phase) and receiver phase. It can also be disturbed by pressure differences across the two aqueous phases. However, ELM is quite difficult to prepare and after metal ion extraction into the emulsion, the oil droplets need to be separated and broken up to recover the receiving phase. Compared to the BLM, the ELM is cumbersome to operate. SLM, viz. a flat sheet (FSSLM) or a hollow fibre (HFSLM) involves a porous polymeric support with its pores filled with the organic solvent which acts as membrane. The HFSLM essentially employs capillary membranes as the medium of separation of feed and receiver phases. It has the potential to be employed on industrial scale separations, including different stages of nuclear fuel cycle. These include recovery of metals from hydrometallurgical leach solutions, treatment and concentration of low-level aqueous waste from reprocessing plants, actinide partitioning from aqueous raffinate waste streams generated after plutonium recovery operations in the PUREX process or from waste streams of radiochemical laboratories engaged in analytical and research activities.

Permeation of metal ions across HFSLM

The HFSLM system with the feed and strip flow directions is shown in Fig. 1. The mass transfer reaction through liquid membrane involves extraction of metal ions at aqueous feed–membrane interface, diffusion of the metal-ligand complex inside the

membrane pores, and finally, dissociation of the metal-ligand complex at membrane–aqueous strip interface (stripping). To improve the permeability and selectivity of the transported species, one has to use a selective ligand with satisfactory D_M (distribution coefficient) value, high D_0 (membrane diffusion coefficient) value and minimum membrane thickness. The idea of using thin organic layer separating two aqueous phases (as in the case of SLM) seems very attractive because the D_0 value in liquids is several times higher than in solid polymer and inorganic membranes.

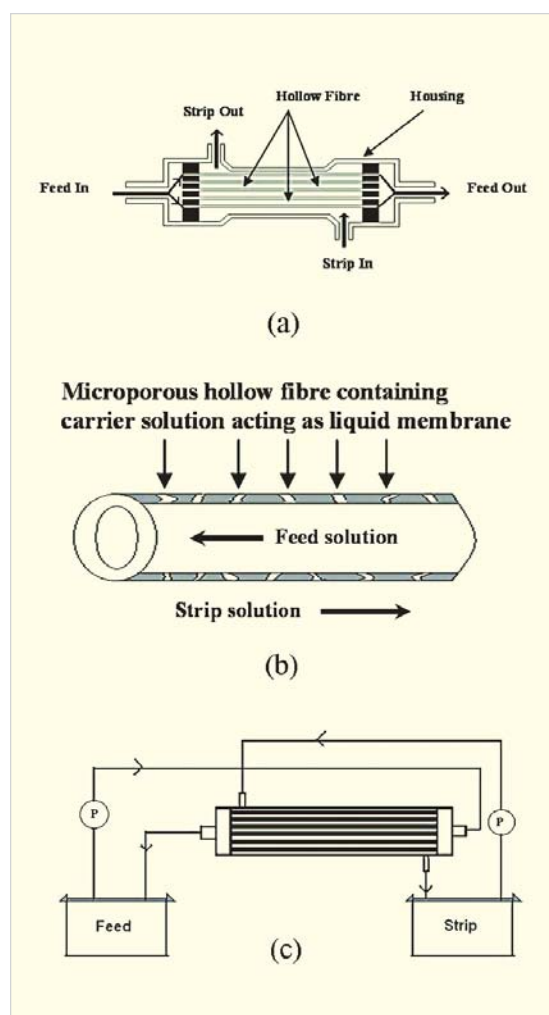


Fig. 1: Schematic representation of hollow fiber liquid membrane; (a) Hollow fibre module, (b) Flow pattern in HFSLM, and (c) HFSLM transport assembly

Separation studies using HFSLM

We have used HFSLM technique for the successful separation of valuables on lab-scale for possible application of the technique in the back-end of the nuclear fuel cycle. Our studies include separation of minor actinides such as Am, and recovery of ^{137}Cs from simulated HLW, separation of ^{90}Y from ^{90}Sr and recovery of U & Pu from analytical wastes.

Actinide partitioning studies

During the last few decades, several extractants have been developed for actinide partitioning. Amongst them TRUEX solvent (0.2 M CMPO + 1.2 M TBP) and DIAMEX solvent (1 M DMDBTDMA) have been extensively studied for moderate acidic (3-4 M HNO_3) waste solution. On the other hand, diglycolamide extractants have been the recent focus of many groups working in the field of actinide partitioning. It was interesting, therefore, to compare the performance of these solvents in HFSLM system. The transport of Am(III) was investigated in the presence of 0.6 g/L Nd (estimated total concentration of lanthanides in PHWR-HLW) and the results are shown in Fig. 2(a). For TODGA and TEHDGA systems, quantitative transport of Am(III) was achieved in 30 min.^{5,6} Significantly fast transport can be correlated to their large distribution coefficient for Am(III). At moderate acidity (3-4 M HNO_3), the D_{Am} value by diglycolamide extractants are sufficiently large (>100) to shift the equilibrium reaction (1) quantitatively to the forward direction, thereby facilitating extraction of metal-ligand complex at aqueous feed-membrane interphase. Similarly, the D_{Am} values at lower acidity (0.01 M HNO_3) are very low ($\sim 10^{-3}$) which encourage the dissociation of

metal-ligand complex at membrane-aqueous strip interphase. The net effect is fast and quantitative transport of the metal ions by diglycolamide ligands. Under identical conditions of feed and strip solutions, only $\sim 65\%$ Am(III) transport was observed for DIAMEX solvent in 30 min, which was attributed to relatively lower distribution coefficient values of Am(III) by DIAMEX solvent ($D_{\text{Am}} = 10$ at 3 M HNO_3). Similarly, for TRUEX solvent, only 50% transport of Am(III) was noticed in 20 min, beyond which no transport was observed. Investigation of acid transport (Fig. 2(b)) revealed a maximum of ~ 0.5 M HNO_3 transport in 30 min with TODGA, TEHDGA and DMDBTDMA systems. In case of CMPO, however, the strip phase acidity reached to ~ 1 M in 30 min due to presence of relatively large concentration of TBP (1.2 M). The D_{Am} values for TODGA, TEHDGA, DIAMEX and TRUEX solvents at 0.5 M HNO_3 are: 0.2, 0.5, 0.07 and 8, respectively. High distribution ratio in case of CMPO at relatively lower acidity (0.5-1 M) hinders the stripping of metal ions in the receiver phase, which restricts the transport. These results suggest that if CMPO has to be used for the transport of actinides from HLW, acidity of the strip phase needs to be neutralized by adding alkali, periodically.

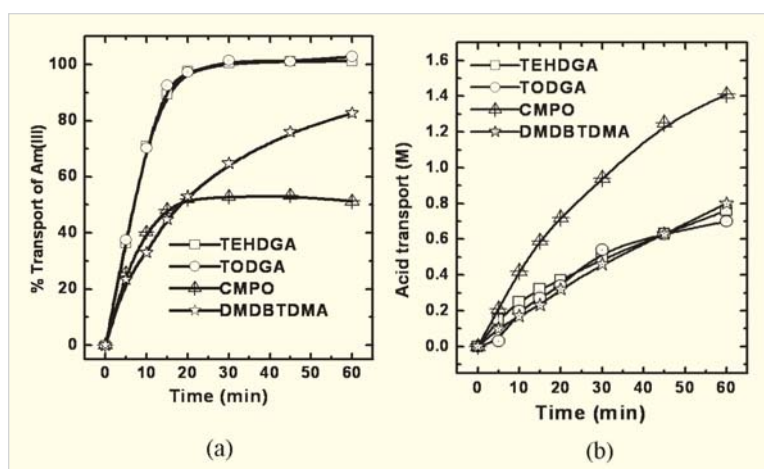


Fig. 2: Transport of (a) Am(III) and (b) acid by HFSLM of different solvents; Carrier: 0.1 M TODGA + 0.5 M DHOA, 0.2 M TEHDGA + 30% isodecanol, 1 M DMDBTDMA and 0.2 M CMPO + 1.2 M TBP; Feed: 0.6 g/L Nd at 3 M HNO_3 (500 mL); Receiver: Distilled Water (500 mL); Flow rate: 200 mL/min.

Pilot scale HFSLM studies

Quantitative transport of Nd was seen in 30 minutes when 0.5 L feed solution containing 0.6 g/L Nd at 3 M HNO₃ was processed using the HFSLM technique. On the other hand, >99% transport of Nd was achieved in 18 h when the operation was performed with 20 L of feed and strip solutions (Fig. 3(a)). The product could be concentrated two times by maintaining the feed to strip volume ratio of 2:1. However,

as the feed to strip volume ratio increased, acid build up in the receiver phase increased significantly which was neutralized by adding NaOH and the acidity of the strip phase was maintained around 0.6 M HNO₃ (Fig. 3(b)). The final composition of the two times concentrated product was: 1.2 g/L Nd + 0.2 M NaNO₃ at 0.9 M HNO₃, which was suitable for the lanthanide actinide separation after suitable neutralization of the feed as demonstrated earlier in our laboratory using Cyanex-301 as the extractant.⁷ With this encouraging result, the transport was studied using 20 litres of SHLW as feed and distilled water as receiver phase (20 litres). It was found that all the lanthanides were

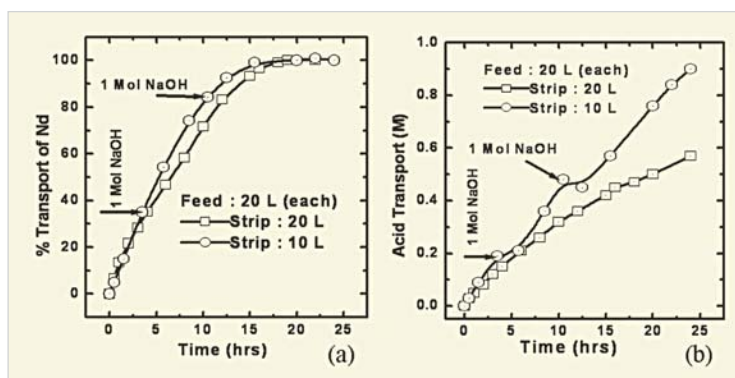


Fig. 3: Transport of (a) Nd and (b) acid by HFSLM; Carrier: 0.1M TODGA + 0.5 M DHOA, Feed: 0.6 g/L at 3 M HNO₃ (20 L); Strip: Dist. water; Flow rate: 200 mL/min. Arrow indicates the point of addition of 1 Mol NaOH.

quantitatively transported in 18 h. As summarized in Table 1, none of the other metal ions were transported along with lanthanides, except Sr and Mo which were co-transported to ~5-10%. The present work reveals the potential of TODGA-HFSLM system for the recovery of actinides and lanthanides from HLW solution.

Lanthanide / Actinide separation

The strategy of P&T (Partitioning of long-lived radionuclides followed by Transmutation) envisages the complete removal of minor actinides from radioactive waste and their subsequent burning in the reactors/ accelerators as mixed oxide fuel. Since,

Table 1: Transport of metal ions from PHWR-SHLW by TODGA-HFSLM after 18 hrs; Carrier: 0.1 M TODGA + 0.5 M DHOA in NPH; Feed: SHLW at 3 M HNO₃ (20 L); Strip: Distilled water (20 L); Flow rate: 200 mL/min

Elements	Conc., (g/L)	% Transport	Elements	Conc., (g/L)	% Transport
Na	5.50	ND	Mo	0.14	8.9
K	0.22	ND	Cs	0.32	ND
Cr	0.12	ND	Ba	0.06	ND
Mn	0.43	ND	La	0.18	>99.9
Fe	0.72	ND	Ce	0.06	>99.9
Ni	0.11	ND	Pr	0.09	>99.9
Sr	0.03	6.9	Nd	0.12	>99.9
Y	0.06	>99.9	Sm	0.086	>99.9

ND : Not detectable

lanthanides and actinides are separated together in the actinide partitioning step, the presence of former would affect the transmutation of actinides due to large neutron absorption cross section of lanthanides (present in large excess over minor actinides) and possible interference during target fabrication where they may form a separate phase. It is necessary, therefore, to separate lanthanides from the actinides before their transmutation. However, it is quite a challenge for the chemical separation of trivalent lanthanides from the trivalent actinides due to their similar chemical properties. Bis(2,4,4-trimethyl pentyl) dithiophosphinic acid (Cyanex-301) has shown promise for the separation of trivalent actinides from their lanthanide counterparts⁸. Unusually high S.F. of ~40,000 has been reported by us for Am(III) / Eu(III) separation using synergistic mixture of Cyanex-301 and o-phenanthroline / 2,2'-bipyridyl.⁸ The feed solution was 500mL containing mixture of lanthanides (1 g/L spiked with tracers such as ¹⁴⁰La, ¹⁶⁰Tb, ¹⁶⁶Ho, ¹⁷⁵Yb and ¹⁷⁷Lu) along with ²⁴¹Am tracer at 1 M NaNO₃ buffered at pH 3.5 with sulphanic acid. The strip solution was 500 mL of 0.01 M EDTA at pH 3.5. It was observed that quantitative (>99.9%) transport of Am(III) was possible in 10 min with 0.5 M Cyanex-301 as the carrier with almost negligible presence of lanthanides. The decontamination factors for all the lanthanides were ~100 making this one of the most promising separations using HFSLM.

Recovery of Cs from radioactive waste

Cesium is one of the important radionuclides arising from the fission of ²³⁵U in the nuclear reactors. ¹³⁵Cs ($t_{1/2} = 2.3 \times 10^6$ years) and ¹³⁷Cs ($t_{1/2} = 30.1$ years) are major isotopes of Cs present in HLW). Separation of radio-caesium from the HLW is important from the safe radioactive waste management point of view. In addition, ¹³⁷Cs has enormous applications as radiation source. Calix[4]arene-bis-crown-6 molecules in 1,3-alternate conformation are reported to be extremely selective for Cs in the presence of

large concentrations of Na.⁹ The excellent separation of radio-caesium was obtained with calix[4]arene-bis-2,3-naphtho-crown-6 (CNC) as the carrier using HFSLM technique. The transport of Cs(I) and other metal ions present in HLW (Cr, Fe, Sr, Am and Eu, etc.) was investigated on 0.5 L scale by calixcrown-HFSLM from a feed solution of 3 M HNO₃ into distilled water.¹⁰ With 1 mM CNC as the carrier, quantitative transport of Cs(I) was achieved in 6 h. The selectivity of Cs(I) over other radiotracers (²¹⁴Am, ¹⁵⁴Eu, ^{85,89}Sr, ⁵⁹Fe and ⁵¹Cr) was excellent with decontamination factors of ~100 w.r.t. various metal ions investigated. High decontamination factors as well as throughputs suggested possible application of the system for the recovery of radio-caesium from high level waste.

Separation of Sr and Y

Yttrium-90 ($t_{1/2} = 64.1$ hrs) has therapeutic applications in various radiopharmaceuticals. Y-90 is usually recovered by milking from Sr-90 ($t_{1/2} = 28.8$ yrs) which undergoes beta decay to produce daughter Y-90 isotope. Acidic organophosphoric acid extractants such as 2-ethylhexylphosphonic acid-2-ethyl hexylmonoester (PC88A) has been used for the recovery of trivalent lanthanide and actinide ions from relatively lower acidic (~0.1 M HNO₃) feed condition. It has been also used for the separation of Y-90 from Sr-90.¹¹ In the present work, Sr/Y separation was carried out at 500 mL scale by HFSLM technique using PC88A as a selective carrier for Y. The feed solution was 0.1 M HNO₃ containing Sr-90/Y-90 mixture, and the strip solution was 3 M HNO₃. Selective permeation of Y was observed and quantitative transport could be achieved in ~30 minutes.¹² On the other hand, transport of Sr was negligible in the receiver phase in this time period. The purity of the separated Y-90 was ascertained by the half-life measurement which was found to be fairly pure with half-life of 64.4 h as compared to the pure tracer which has half-life of 64.1 h.

Recovery of Pu from Analytical Waste

Chemical laboratories of fuel reprocessing / fabrication of Pu-based fuels (engaged in process control, material accounting and quality control) generate analytical wastes where it is mandatory to recover Pu and Am to facilitate safe disposal of the waste effluent. Typically, major impurities are Na, Fe, Ca, Al, Cr, Mg, Ni and Zn. Conventionally precipitation and ion exchange procedures are employed for the recovery of Pu, which generate large volume of liquid waste in glove-box operations. In addition, personal dose to the operator due to ^{241}Am (daughter product of ^{241}Pu) need to be accounted. At Radiochemistry Division, HFSLM technique has been demonstrated for the first time on litres-scale for the recovery of plutonium from analytical acidic waste using 30%TBP / *n*-dodecane as the carrier.

The recovery of Pu from the waste was carried out in two stages. In the first stage, Pu(IV) and U(VI) were selectively transported into the receiver phase by TBP-HFSLM. The feed solution was a mixture of 3.22 g/L Pu, 110 g/L U and 60.2 mg/L Am. Pu was adjusted to +4 state using NaNO_2 at 3 M HNO_3 . About 96.2% U and 97.9% Pu was selectively transported into the receiver phase in 3 h. The Am(III) contamination in the product (U and Pu fraction) was found to be $<0.1\%$. In the subsequent stage, in the feed solution containing U and Pu, the valency of Pu was adjusted to Pu(III) (by 1:1 hydroxylamine and hydrazine hydrate) while the acidity was kept at ~ 1 M HNO_3 . The TBP-HFSLM cycle was carried out using 0.1 M Na_2CO_3 as the receiver phase. Analysis of the feed and the receiver phases after 1 h suggested 89.7% U transport into the receiver phase. In order to remove U completely from the Pu fraction, the strip solution was replaced with equal volume of fresh receiver phase (1 L of 0.1 M Na_2CO_3) and the system was run for another one hr. Final results suggested that $>99\%$ Pu remained in the feed solution with about 0.5% contamination from U. Samples of the recovered plutonium and

uranium from the analytical laboratory waste are shown in Fig. 4. Analysis of common metallic impurities in the Pu fraction was carried out by ICP-AES and the results indicated high DF values suggesting 99% of both U and Pu. By following the above procedure, about 50 g Pu could be recovered from 10 litres of analytical waste.

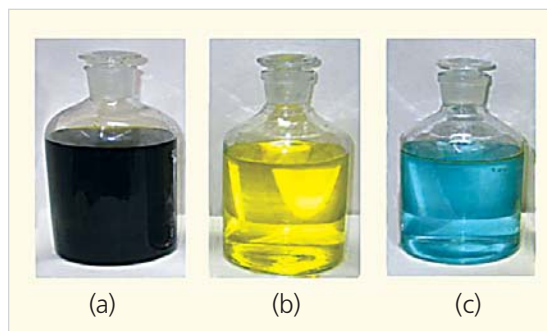


Fig. 4: The recovered plutonium and uranium from the analytical waste; (a) waste solution, uranium solution and (c) plutonium solution

Stability of HFSLM

The long term stability of the HFSLM is important from the standpoint of its industrial application. For physical stability of the HFSLM, the module was impregnated once with the carrier solution (0.1 M TODGA + 0.5 M DHOA / NPH) and the system was operated continuously in eight successive cycles for the transport of Nd from a feed solution containing 1 g/L Nd at 3 M HNO_3 (500 mL). It was encouraging to note that the Nd transport was consistent within the error limits in all the eight runs. Similarly, the system was continuously operated for 72 h when no change in the transport of Nd was observed, suggesting good stability of the HFSLM system. Danesi, et al.¹³ reported that the loss of carrier from the pores is more significant when carrier molecules are very strong surfactant such as alkyl / aryl sulphonic acids and long chain quaternary ammonium salts. On the other hand, no significant loss was observed when weaker surface active carriers such as CMPO, TOPO and long chain amines were used. In the present work, TODGA being a weaker surface active carrier, is

expect to have similar stability. The radiolytic studies of the carrier (0.1M TODGA + 0.5 M DHOA in NPH) revealed an excellent stability of the carrier up to 500 kGy. The radiation stability of the hollow fibre module (1"x 9" module) was also investigated by irradiating it up to 500 kGy and measuring of the transport rates of Nd. The transport data reflected excellent reproducibility of the results, suggesting excellent radiation stability of the hollow fibre upto ~500 kGy. However, the body of the module as well as the fibers became brittle at >500 kGy dose. SEM pictures of the fibers before and after irradiation are shown in Fig. 5. It is necessary, therefore, to develop radiation resistant polymers for long term use of HFSLM technique for radioactive waste remediation.

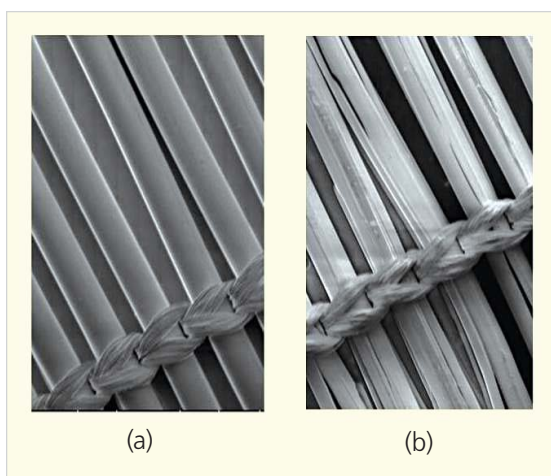


Fig. 5: SEM pictures (Magnification 200X) of the hollow fiber lumens before (a) and after (b) irradiation (500kGy).

Conclusions

Quantitative transport of trivalent actinides and lanthanides was demonstrated from SHLW using hollow fibre supported liquid membrane (HFSLM) technique. A mixture of 0.1 M TODGA + 0.5 M DHOA was found to be a suitable carrier where quantitative transport of trivalent actinides and lanthanides was achieved within 30 minutes from PHWR-SHLW on 500 mL scale. On the other hand,

~18 h were necessary for a similar transport on 20 litres scale. Physical and chemical stability of TODGA-HFSLM was demonstrated to be excellent for 72 h of continuous operation. Radiation stability of the carrier (0.1 M TODGA + 0.5 M DHOA) and hollow fibre lumen was satisfactory at ~500 kGy dose. The transport behaviour of trivalent actinides and lanthanides by TODGA-HFSLM was compared with other proposed extractants for actinide partitioning, viz. TEHDGA, TRUEX and DIAMEX solvents. For different solvents, the transport followed the order: 0.1 M TODGA + 0.5 M DHOA ~ 0.2 M TEHDGA + 30% *iso*-decanol > 1M DMBTDMMA > 0.2 M CMPO + 1.2 M TBP. This order was explained on the basis of co-transport of acid and the distribution ratio of metal ions at the acidity encountered in the strip phase. The HFSLM technique was successfully applied for the selective recovery of trivalent actinides over lanthanides using Cyanex-301 as the carrier. Similarly, the technique could be successfully applied for the separation of ^{90}Y from ^{90}Sr using PC88A as the carrier. The HFSLM technique was also applied on process scale for the recovery of radio-caesium, which revealed selective recovery of Cs(I) over other metal ions, viz. Am, Eu, Sr, Fe and Cr with decontamination factors of ~100. High decontamination factors as well as throughputs suggested possible application of the system for the recovery of radio-caesium from high level waste.

The present studies revealed that HFSLM technique offers a promising alternative approach for nuclear waste remediation. The basic phenomena governing the HFSLM process are similar to SLM and are sufficiently well understood to permit the scale-up of laboratory units.

References

1. Hayworth, H.C., Ho, W.S., Burnes, W.A. Jr., Li, N.N.; *Sep. Sci. Tech.*, 18 (1983): 493-521.
2. Ansari, S.A., Bhattacharyya, A., Raut, D.R., Mohapatra, P.K., Manchanda, V.K.; *Radiochim. Acta*, 97 (2009): 149-153.

3. Ansari, S.A., Mohapatra, P.K., Manchanda, V.K.; *Ind. Eng. Chem. Res.*, 48 (2009): 8606-8612.
4. Mohapatra, P.K., Manchanda, V.K.; *Ind. J. Chem.*, 42A (2003): 2925-2939.
5. Ansari, S.A., Mohapatra, P.K., Raut, D.R., Seshagiri, T.K., Rajeswari, B., Manchanda, V.K.; *J. Membr. Sci.*, 337 (2009): 304-309.
6. Ansari, S.A., Mohapatra, P.K., Raut, D.R., Adya, V.C., Tulsidas, S.K., Manchanda, V.K.; *Sep. Purif. Technol.*, 63 (2008): 239-242.
7. Bhattacharyya, A., Mohapatra, P.K., Ansari, S.A., Raut, D.R., Manchanda, V.K.; *J. Membr. Sci.*, 312 (2008): 1-5.
8. Zhu, Y., Chen, J., Jiao, R.; *Solv. Extr. Ion Exch.*, 14 (1996): 61-69.
9. Asfari, Z., Wenger, S., Vicens, J.; *Pure and Applied Chemistry*, 67 (1995): 1037-1043.
10. Kandwal, P., Mohapatra, P.K., Ansari, S.A., Manchanda, V.K.; *Radiochim. Acta*, 98 (2010): 493-498.
11. Ramanujam, A., Achuthan, P.V., Dhami, P.S., Kannan, R., Gopalakrishnan, V., Kansra, V.P., Iyer, R.H., Balu, K.; *J. Radioanl. Nucl. Chem.*, 247 (2001): 185-191.
12. Kandwal, P., Ansari, S.A., Mohapatra, P.K., Manchanda, V.K.; *Sep. Sci. Technol.*, 46(2011): 904-911.
13. Danesi, P.R.; *Sep. Sci. Technol.*, 19 (1985): 857-894.

Modeling of Deformation Behaviour of HCP Metals using Crystalplasticity Approach

A. Sarkar and J.K. Chakravartty

Mechanical Metallurgy Division, Materials Group

Abstract

The viscoplastic self-consistent (VPSC) formulation is by now a well established approach for simulating texture development and constitutive response during plastic formation of high and low-symmetry polycrystals. In this work we have used the VPSC approach to model the uniaxial tensile and compressive deformation characteristics of pure magnesium and Zircaloy-2. We compare our results with experimental data and find that they are in good agreement with the available experimental data.

Introduction

A piece of metal is normally made up of millions of crystallites or grains arranged in an unknown, complex and irregular 3-dimensional aggregate. Individual crystallites are single crystal having particular crystallographic orientation. The distribution of orientation of individual grain in a polycrystalline material is an important microstructural feature. It affects the overall physical and mechanical properties of the material. If the distribution of orientations is inhomogeneous, the material is called to have crystallographic texture.

The computation of the macroscopic response of polycrystalline aggregates from the properties of their constituent single-crystal grains is one of the main problems in the mechanics of materials. When a polycrystalline material undergoes mechanical processing, each crystal is reoriented. The polycrystal may thus develop a crystallographic texture which is particularly responsible for the material anisotropy. It is therefore important to model the texture development in polycrystals to include anisotropy effects that are present in many industrial processes. The formulation of the plasticity of metallic

polycrystals has been a subject of many studies and different approaches have been proposed. The main crystal plasticity models for large deformation are: Taylor-type¹, Sachs-type², self consistent models³. These models are based mainly on the physical deformation mechanisms of slip and twinning, the two important modes, and account for hardening and reorientation of single-crystal grains. Crystal plasticity models vary in the degree of sophistication used to describe the interaction of each grain with its surrounding. Both the upper bound Taylor and the lower bound Sachs models ignore the interactions among the grains. Self-consistent models can be used to account for intergranular heterogeneities during plastic deformation of polycrystals.

Viscoplastic self-consistent (VPSC) formulation

In the VPSC model each grain is assumed to be an ellipsoidal visco-plastic inclusion in a homogeneous effective medium (HEM); the HEM is treated as a textured anisotropic plastic aggregate. The interaction between the grain and the HEM is carried out by a visco-plastic Eshelby approach. The model iterates to a solution where the HEM represents the average

response of the grain population used. Deformation is based on crystal plasticity mechanisms – slip and twinning systems – activated by the resolved shear stress. The single crystal response is described by means of a rate sensitive constitutive law of the form:

$$\dot{\epsilon}_{ij} = \sum_s m_{ij}^s \dot{\gamma}^s = \dot{\gamma}_0 \sum_s m_{ij}^s \left(\frac{m^s : \sigma}{\tau^s} \right)^n = M_{ijkl} \sigma_{kl} \quad (1)$$

Where $\dot{\epsilon}$ is the strain rate in the grain, s labels each slip and twinning system, m^s is the geometric schmid tensor, τ^s is a threshold stress controlling the activation of the system, and n is the inverse of the rate sensitivity. At the aggregate level, overall strain rate and stress are related through either a secant or tangent constitutive law. A full description of this formalism can be found in Ref. 3.

In the model, the evolution of threshold stress (τ^s) of individual deformation modes is described with an empirical Voce hardening law:

$$\tau^s = \tau_0^s + (\tau_1^s + \theta_1^s \Gamma) \left(1 - \exp\left(-\Gamma \frac{\theta_0^s}{\tau_1^s}\right) \right) \quad (2)$$

Where τ_0^s and $(\tau_0^s + \tau_1^s)$ are the initial and final back extrapolated Critical Resolved Shear Stress (CRSS) respectively. θ_0^s and θ_1^s are the initial and asymptotic hardening rates and Γ is the accumulated plastic shear in the grain. The model also allows for the possibility of self and latent hardening.

Activity of different deformation modes (slip and twin) during plastic deformation of hcp materials is primarily governed by the c/a ratio of the hexagonal lattice. To elucidate this effect, we have chosen two systems with different c/a ratio: namely Magnesium ($c/a \approx 1.624$) and Zircaloy-2 ($c/a \approx 1.590$).

Simulation on Magnesium

Magnesium alloys have attracted great attention in recent years due to their potential application in the automobile industry for improving fuel efficiency through vehicle weight reduction. One problem that inhibits widespread application of magnesium alloys is limited ductility and, in particular, poor room temperature formability of the current commercial alloys. Moreover, Mg and its alloys exhibit strong deformation anisotropy. The mentioned mechanical anomalies of magnesium originate from its micromechanical deformation mechanisms, which are determined by its hcp crystallographic structure. Metals with hcp structures have reduced number of available slip systems compared to cubic structures, making plastic deformation more difficult. Various primary and secondary slip and twinning mechanisms can be activated at the same time during the deformation of the hcp materials. Therefore, modeling of the macroscopic deformation of hcp materials requires a careful investigation of the micromechanisms. Understanding the mechanisms of dislocation gliding and deformation twinning for single crystals and polycrystalline aggregates constitutes the foundation for modeling of the macroscopic mechanical behavior.

C.H. Ca´ceres and A.H. Blake⁴ carried out compression and tensile tests on random Magnesium polycrystal. In this work we have used these data to model the deformation characteristics of Mg. To start with we generate 1000 grains with random orientations. Deformation is based on crystal plasticity mechanisms – slip and twinning systems – activated by the resolved shear stress. The plastic deformation mechanisms observed in Mg and its various alloys include slip in $\langle a \rangle$ - direction $\{0001\} \langle 11\bar{2}0 \rangle$ basal slip, $\{1\bar{1}00\} \langle 11\bar{2}0 \rangle$ prismatic slip, slip in $\langle a+c \rangle$ -direction $\{11\bar{2}2\} \langle 11\bar{2}3 \rangle$: pyramidal slip and tensile twinning $\{10\bar{1}2\} \langle 10\bar{1}1 \rangle$. We have activated these four different deformation modes to match the simulated stress-strain curve with the experimental

Table 1: Hardening parameters of the different deformation modes for Magnesium

Deformation mode	τ_0 (MPa)	τ_1 (MPa)	Θ_0 (MPa)	Θ_1 (MPa)
Basal <a>	16	60	120	0
Prismatic <a>	35	40	150	0
Pyramidal <c+a>	45	80	800	0
Tensile Twin	8	0	30	30

Table 2: Hardening parameters of the different deformation modes for Zircaloy-2

Deformation mode	τ_0 (MPa)	τ_1 (MPa)	Θ_0 (MPa)	Θ_1 (MPa)
Prismatic	20	15	1285	80
Pyramidal	150	190	1685	5
Tensile Twin	100	15	95	25
Comp Twin	275	30	950	175

data. The values of the hardening parameters for the best fit of the compression and the tensile deformation curves are shown in Table 1.

Experimental and simulated uniaxial compression and tension curves (stress vs plastic strain) for Mg with random texture are shown in Fig. 1. It can be seen that the simulated curves match very well the experimental data. Relative activities of the four different deformation modes used in the simulation are shown in Fig. 2.

Simulation on Zirconium alloy

Zirconium has been reported to deform by a variety of modes: prismatic <a>, pyramidal <c + a> and basal slip <a>, two types of tensile twinning: $\{10\bar{1}2\} <10\bar{1}1>$ and $\{11\bar{2}1\} <11\bar{2}\bar{6}>$ and two types of compression

twinning: $\{11\bar{2}2\} <11\bar{2}\bar{3}>$ and $\{10\bar{1}1\} <10\bar{1}\bar{2}>$ ⁵. The active modes and their relative contribution to deformation depend on strain level, temperature, strain rate, direction of loading, and purity level. Deformation is further complicated by the fact that each mode has its own sensitivity to temperature and strain rate. Understanding the deformation behavior of Zr (texture evolution, plastic anisotropy, hardening rate) requires not only knowing

which of these mechanisms operate, but also how they interact to produce desired plastic strain.

The material used in this study is rolled and annealed Zircaloy-2 plate. Fig 3a. shows the pole figures of the starting material in annealed condition.

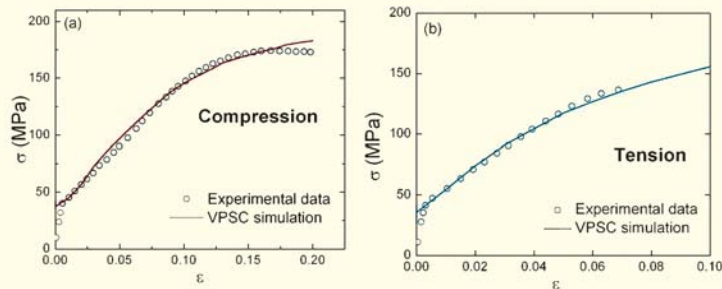


Fig. 1: Experimental and simulated uniaxial (a) compression and (b) tensile curves

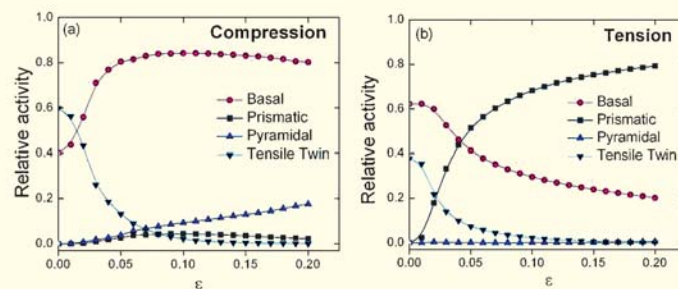


Fig. 2: Relative activities of different slip and twin systems during (a) compression and (b) tension of Mg

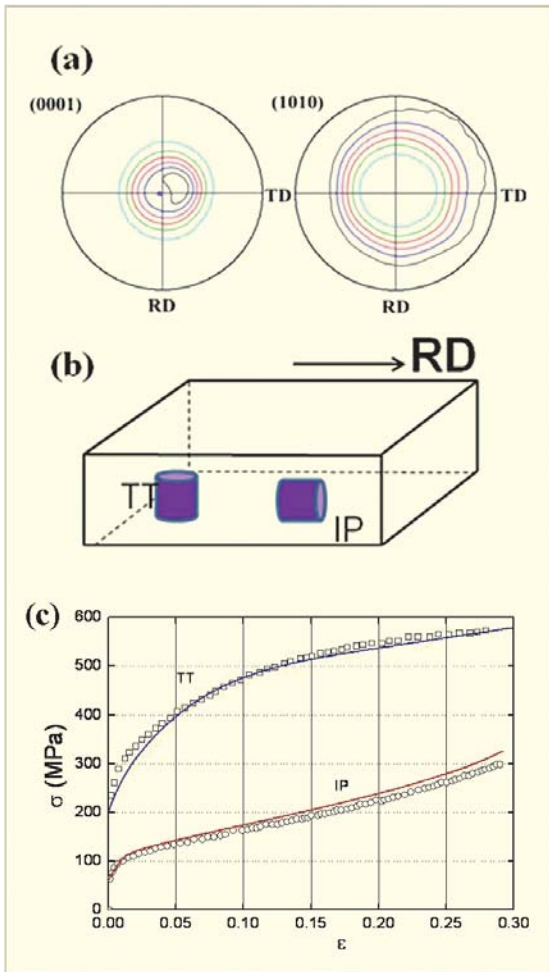


Fig. 3: (a) Pole figures of the starting material (b) schematic of the samples (c) experimental and

Compression samples have been fabricated from the rolled sheet in the through thickness (TT) and in-plane (IP) directions as shown in Fig 3b. The samples were deformed in uniaxial compression at a strain rate of 0.001/s. Fig 3c shows the experimental stress strain curves. Flow curves were modeled using VPSC approach. Two slip and two twin systems (Table 2) have been activated to match the simulated stress-strain curve with the experimental data. The values of the hardening parameters for the best fit of the flow curves are shown in Table 2. It can be seen in Fig 3c that the simulated curves match very well the experimental data. Relative activities of the four different deformation modes used in the simulation are shown in Fig. 4.

Conclusion

Deformation characteristics of hcp materials (Mg and Zircaloy-2) have been modeled using the VPSC approach. Our study revealed that the tensile and compressive flow curves of Mg can be well modeled considering the four deformation modes and their activation: three basal slip systems, three prismatic slip systems, six pyramidal slip systems and six tensile twinning systems. (Table 1 is the explanation of this conclusion) It is found that the basal slip is the

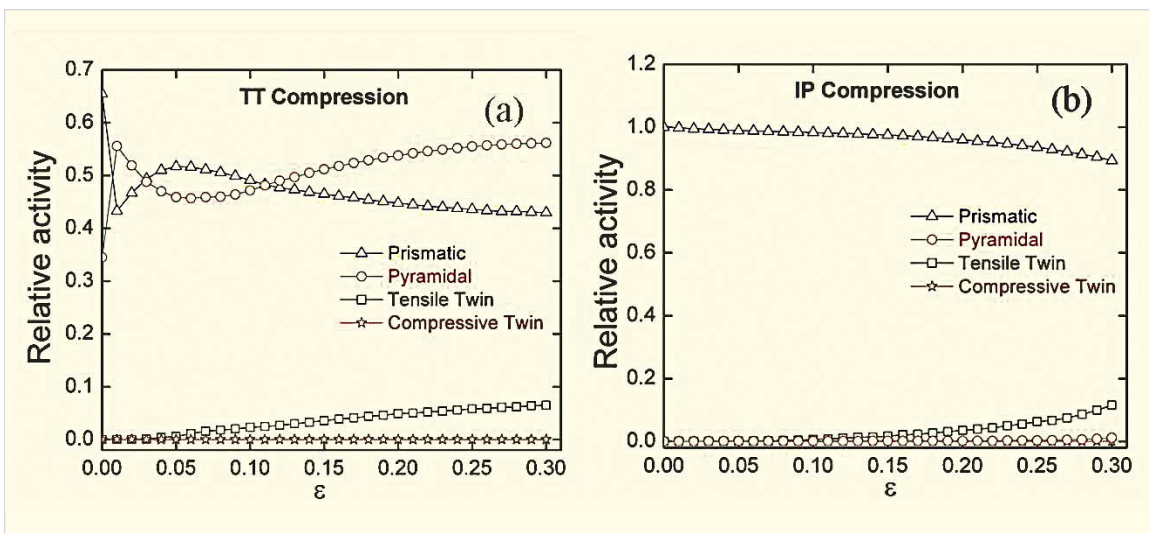


Fig. 4: Relative activities of different slip and twin systems during (a) TT and (b) IP compression of Zircaloy

primary deformation mode in case of compression while the prismatic slip takes the leading role in tensile deformation. In case of Zircaloy-2 the flow behaviour depends on the sample orientation. Two slip and two twin system were activated to simulate the flow behavior of two samples with different orientation. These results establish the efficacy of the VPSC approach to model the plastic deformation behavior of hcp materials.

References

1. Taylor, G.I. "Plastic strain in metals". *Journal of the Institute of Metals* 62 (1938): 307-324.
2. Sachs, G. "Zur Ableitung einer Fließbedingung". *Zeitschrift der Verein deutscher Ingenieur* 72 (1928): 734-736.
3. Lebensohn, R.A., Tome', C.N. "A self-consistent anisotropic approach". *Acta Metallurgica et Materialia*, 41 (1993): 2611–2624.
4. Cáceres C.H., Blake A. H. "On the strain hardening behaviour of magnesium at room temperature". *Materials Science Engineering A* 462 (2003): 193-196.
5. Beyerlein, I.J., Tomé, C.N. "A dislocation-based constitutive law for pure Zr including temperature effects". *International Journal of Plasticity* 24 (2008): 867-895.

Forthcoming Symposium

DAE Solid State Physics Symposium(DAE-SSPS)

DAE-SSPS, the 56th in the series, will be held at the SRM University, Kattankulathur, Tamil Nadu, during Dec 19-23, 2011. It is sponsored by the Board of Research in Nuclear Sciences, DAE, Government of India. This symposium is a very popular and prestigious scientific event, bringing together research students and scientists from across the country.

This is the first announcement.

For further details you may contact:

Convener

Prof. R. Mukhopadhyay
BARC, Mumbai
Email: mukhop@barc.gov.in
Tel. +91-22-25594667

Local Convener

Prof. J. Thiruvadigal
Head, Department of Physics
SRM University
Kattankulathur - 603203
Tamil Nadu
Email:hod.ph@ktr.srmuniv.ac.in

A Material Transfer System using Automated Guided Vehicles

R.V. Sakrikar, P.V. Sarngadharan, S. Sharma, V.K. Shrivastava, A.P. Das,
V. Dave, N. Singh, P.K. Pal and Manjit Singh

Division of Remote Handling & Robotics

Abstract

This article describes an implemented solution for the material distribution problem in the machining shop of a typical manufacturing unit using Automated Guided Vehicles (AGV). We briefly describe the AGV and its associated material handling system, and then go on to describe the software components and their underlying algorithms, which, when put together, create an automated material transfer system that assesses demands for materials and accordingly plans, prioritizes and executes deliveries. The system has been tested extensively in a mock environment in our Laboratory, the results for which have also been indicated here.

Introduction

Manufacturing requires continuous movement of materials – starting from the point where vendors deliver semi-finished components, up to the point where the finished products are ready for shipment. In between, the semi-finished components are moved to various machining units, to assembly station, testing and quality control, packaging, and so on until the product is complete in all respects. In the past, these movements were performed manually. The idea of deploying one or more Automated Guided Vehicles (AGV) for this purpose is gaining in popularity these days, because they have the potential of making all movements in the manufacturing unit completely autonomous, safe, and extremely efficient, leading to higher productivity and automatic storage management eventually at a lower cost. All that is required is one or more vehicles that can move and stop precisely along designated trajectories, material transfer mechanisms like powered roller conveyors, and proximity sensors to know the presence and absence of materials on the conveyors. A set of computer programs can then take care of the entire material

transfer operations. That adds to its flexibility; the entire plan can be changed at will by editing trajectories and a few other parameters.

Since the requirement for movement of materials is generic, the need for an automated material transfer system is felt by all segments of industries; more so by those whose processes are well structured to take advantage of automation, or those who are keen to avoid manual handling of hazardous (e.g., radioactive or explosive) materials. The available imported solutions turn out to be very expensive, as in each case they need to be customized to meet exact requirements of the industry. The development of Automated Material Transfer System (AMTS) was taken up at DRHR, BARC, to generate an indigenous solution that is affordable to the Indian industries going for modernization of their manufacturing processes, and that can be adapted to the exact requirements of an industry without adding substantially to its cost. The solution can also be readily adapted to automated handling and shipment of radioactive materials in the nuclear establishment.

As a concrete instance around which we can make initial development of the AMTS, we selected the

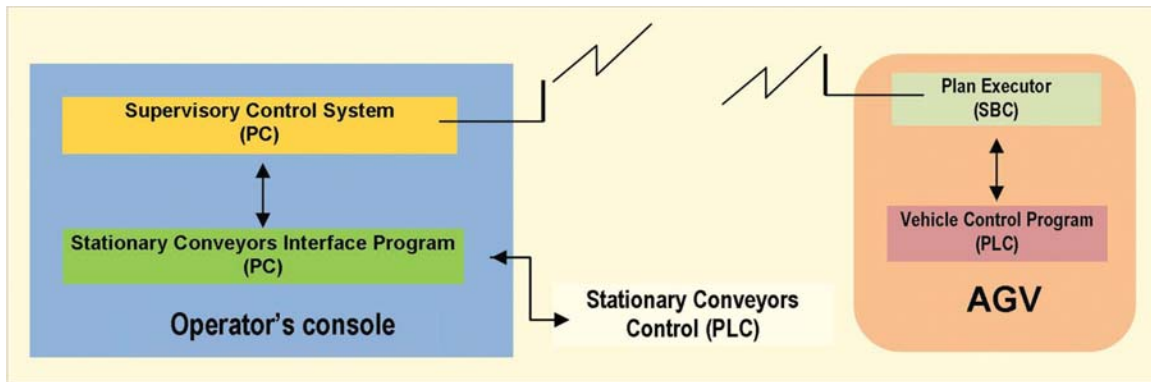


Fig. 1: AMTS Control Architecture

problem of automation of the transfer of semi-finished components, from a supply point to several machining centres on the shop floor of a typical manufacturing setup. The semi-finished components are packed into bins, which are stacked up for transfer to and from the AGV. The complete stack is handled by the system and delivered at the designated locations. The automation system so developed has the ability to be scaled to use and control multiple AGVs if the situation demands.

Fig. 1 shows the overview of the control architecture of the AMTS [1]. The vehicle is controlled by a Vehicle Control Program (VCP) running on a PLC on the AGV under the guidance of a Plan Executor (PE) program running on an onboard single board computer. PE executes plans for transfer orders prepared and assigned by the Supervisory Control Program to the AGV. The Supervisory Control Program runs on a stationary PC located conveniently in the Control room or Shop Floor. This program displays current status of the AGV and loading /unloading stations. It allows an operator to set transfer orders for materials, or to intervene through Emergency-Stop. A stationary PLC in the shop-floor controls all the conveyors in the loading /unloading stations. These are described in more detail in the following sections.

Autonomous Guided Vehicle (AGV)

An AGV is a battery powered mobile platform with the ability to interpret and execute a set of motion

commands. This is achieved through appropriate design and control of the vehicle as detailed below.

Mechanical Design

In a shop floor, it is desirable for the AGV to move along straight paths, curves, turn in place (around its centre) and crab (shift parallel to itself). In order to cater to these requirements, the *quad* configuration, having two steer & drive wheels mounted on the AGV on the centre-line along its length and four support castors on four corners, has been selected. In addition to satisfying the motion requirements, this configuration has the advantage of low actuator count for high degrees of freedom, thus making the control relatively simple. The general arrangement of the drive wheels and castors are as shown in Fig. 2. The AGV is about 2m long and 1.4m wide, with three rows of conveyors onboard for loading /unloading bins on either side. Its

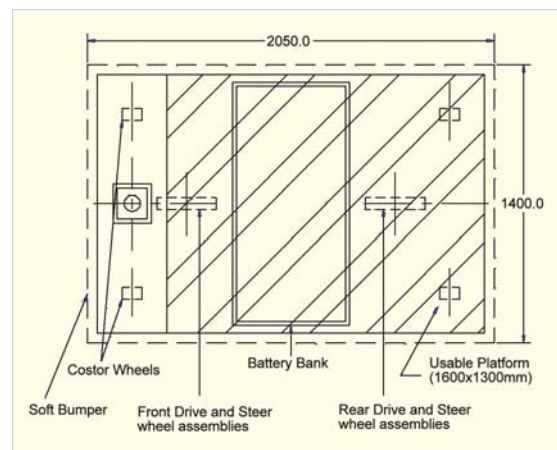


Fig. 2: AGV wheel configurations

payload capacity is about 700kg, and its maximum speed is about 1.3m/s.

Vehicle Control

All the four actuators of the AGV are driven by AC Induction Motors. The control of the motors is achieved using compatible AC Motor Controllers operating on a 48V DC battery supply. The motor controllers provide the velocity loop for the actuators based on the incremental encoders, attached to the motor shaft, as feedback devices. The velocity loop is directly used by the traction actuators for control of wheel speeds. The position control, required for the steer actuators, is achieved by position control PLC module. The position control module takes feedback from the incremental encoders mounted on the motor shaft. The module provides a PI control for maintaining the desired wheel steering angle.

A PLC based Vehicle Control Program (VCP) controls the motion of the AGV. It also controls operation of the onboard material handling system, monitors sensors, compiles AGV status data, and executes operational interlocks. The AGV operations can be controlled either in a program mode, in which it keeps executing commands received from the Plan Executor (PE) module, or in an interactive mode, in which it can be controlled through an operator's pendant mounted on the AGV. The touch panel based operator's pendant also serves as a status display unit during program mode operation.

The AGV can move in three different modes – Tangential, Crab, and Differential. The tangential mode allows tangential motion of the AGV along straight lines and curves. The Crab mode allows movement of the AGV in any direction parallel to itself. While doing that, it additionally allows a small specified correction in the orientation of the vehicle. In the differential mode, the AGV wheels are oriented perpendicular to its length, and all motions like straight, turn-in-place and motion along a curve may be executed by appropriate control of magnitude

and sense of rotation of the two wheels. In programmed mode of operation of the AGV, we use only tangential and crab motions. Differential motion is used mainly for turn-in-place during interactive control of the AGV.

Load Handling Mechanisms

The AGV as well as the loading and delivery stations are provided with motorized roller conveyors for automated transfer of materials to and from the AGV. The AGV conveyors are controlled by the onboard PLC system. The field conveyors have a separate PLC based control system, and the operation of the conveyor sets is coordinated through the Supervisory Control System. Fig. 3 shows the actual AGV with various sub-systems.

Safety

The AGV has a set of bump sensors to be able to stop on contact. Apart from physical safety, the integrity of communication channels between various levels of software is monitored continuously. The AGV is stopped if any breach of safety requirement is detected, and the fault is indicated



Fig. 3: The AGV

to the operator. The AGV so stopped can be put back into the system only with operator intervention after clearing of the faults. A special mode is provided for operation of the AGV under maintenance. The speed of the AGV is limited during such operations.

In order to anticipate and avoid collisions, we are additionally installing a non-contact laser based obstacle detection system, which provides for slowing down or stopping of the AGV depending on the distance of the obstacle much before any contact is established.

Navigation

AGV navigation can be either fixed path or free ranging. In fixed path navigation, the AGV paths are rigidly defined on the shop-floor by using path markers such as magnetic tape, photo reflective tape on the floor or burying of wire below the floor. These methods require compatible sensors on the AGV to detect the paths. This method, however, leads to a rigid system. In case of the free ranging technique, the AGV has a map of the navigation area and several fixed reference points which can be detected by onboard sensors of the AGV. The AGV localizes itself on the basis of perceived locations of these reference points.

Laser Navigator

The present AGV system uses the free ranging technique. It detects cylindrical reflectors installed within the work area through an onboard laser ranging device. The positions of these reflectors are known in advance in a global coordinate system. The laser navigator system returns the position (x, y) coordinates and orientation θ of the laser ranging device with respect to the same coordinate system to the AGV controller at the rate of 8 Hz [2]. The instantaneous position and orientation of the AGV is easily computed from this data.

The navigator system allows definition of a number of convex-shaped overlapping areas of operation of the AGV, comprising various subsets of reflectors to ensure accurate localization in large or poorly connected areas. Each such area is called a layer. The AGV refers to only the most appropriate layer at any instant for its localization.

Trajectory Editor

Systems, which use free ranging techniques, provide high flexibility regarding definition and modification of the work area and AGV trajectories. For this, various entities, such as path segments, branching nodes, loading and unloading stations, reflectors, layers etc., need to be defined. This is done using a system configuration tool called Trajectory Editor (TE). This is a CAD-based software, with the facility to import the layout drawing of the workshop, with outlines of structures, machines and various other entities depicted on it, as a background. TE facilitates creation of routes and loading /unloading stations for the AGV. It runs designated checks on the defined paths, nodes and stations and generates data tables based on the information stored while creating / editing these entities. The trajectory database, so generated by TE, completely describes the system and is loaded on to each AGV in the system. The database is used by Plan Executor (PE) program for navigation of the AGV as per operational attributes over the executing segments. The database is also used by the Supervisory Controller for all its operations including graphical display of system status using workplace drawing.

Plan Executor

The Plan Executor (PE) program, running on the Single Board Computer (SBC) of the AGV, carries out execution of the transfer order placed on the AGV by the supervisory control system. A transfer order is assigned to an AGV only when it is free, i.e., it does not have any pending order to attend to. The transfer order specifies sources from which

materials are to be picked and destinations at which they need to be delivered in a single trip of the AGV. In fact, what PE receives is a detailed plan worked out by the supervisory controller for execution of the transfer order in terms of a chain of nodes and associated activities. On the basis of this plan and the trajectory database, PE computes the actual trajectory to be traversed by the AGV. Accordingly, under the control of a trajectory tracking algorithm (e.g., Pure Pursuit Algorithm, as explained below), it keeps issuing motion and activity commands to the Vehicle Control Program (VCP) running on onboard PLC, until the entire plan gets executed.

The AGV is likely to deviate from its desired trajectory due to inaccuracies in motion control. In order to correct for these deviations, the AGV uses a Pure Pursuit Algorithm [3,4]. This algorithm continuously monitors the position error of the AGV with respect to its reference trajectory and adjusts the curvature of its path in such a way as to reduce the error.

PE gets position data from the Laser Navigator. It also receives vehicle odometer data from the PLC, computed on the basis of traction and steer encoder data. PE uses these data for the purpose of trajectory tracking. The navigator data, being more accurate, is normally used to determine tracking error. The odometer data is used in case the Navigator data is not available for a short duration. PE corrects the PLC odometer data periodically, based on the laser navigator data.

PE receives AGV status information packets at a regular interval (every 100ms) from VCP. The regularity of commands and status packets (heart beat) are continuously monitored by VCP and PE respectively to confirm smooth communication between them. In case the communication fails persistently for some time (1 min), command execution on the vehicle is stopped.

Apart from the above tasks, PE also waits for relevant operator level commands like Emergency-Stop, Join etc., coming from supervisor. It also issues commands to supervisor and PLC for coordinating a loading /unloading operation, apart from keeping the supervisor updated periodically about current AGV status.

Supervisory Controller

It is a computer program executing on a standard desktop computer, located either in the operation area or the control room as per convenience. Its function is to manage one or more AGVs with active infrastructure supports for pick-up and delivery stations. The supervisory control system carries out a range of tasks, namely monitoring of field devices, AGV traffic control, communications and AGV dispatching, tracking and tracing.

Traffic Management & Control

Automatic stopping, starting and routing of AGV is essential to all AGV systems. To ensure against one AGV entering an already occupied zone or intersection of a guide path and to provide for orderly and efficient routing in general, the location of each AGV is monitored and decisions are made based on this knowledge.

In the present system, we have not yet implemented multi-AGV traffic management, as the choice of strategies depend on AGV capacity, transfer load, size and complexity of environment. However, in our developments, wherever possible, we have kept provision for generalizing solutions to multi-AGV case.

Communications

The Communication tasks handled by the supervisory controller include messages, such as issue of transfer order to the AGV, insertion of the AGV into the system, and commands to control field devices in the work area. It also includes fault condition

detection and reporting based on the 'AGV-heart-beat' monitoring. The supervisory controller also monitors the AGV status and takes necessary action based on the information e.g. commanding the AGV to go to the charging station in case of inadequate battery charge. Considering ease of adaptability, large coverage area and flexibility regarding expansion of the coverage area, the Radio frequency based Ethernet communication between the Supervisory Controller and the AGV has been selected.

Communication between the Supervisory Controller and the field devices (e.g., stationary conveyors) is accomplished by using any standard serial protocol over a wired link, as the systems are largely stationary. The operations of the conveyors in loading /unloading stations have to be controlled and synchronized with that on the AGV. A PLC system with distributed I/O is used for this purpose. The PLC communicates with the Supervisory controller on a RS-232 based Modbus interface. The Supervisory controller issues commands for the operation of the conveyors and also for the compilation of the status data for the conveyors. The commands for the conveyor operations are received from the Plan Executor and the activity of the compilation of the status is periodically carried out by the Supervisory controller.

The status data compiled by the controller is further used by the Supervisory Controller for triggering of transfer plans and the information is also passed over to PE as and when required.

Job Generation & Assignment

Job generation and assignment is an essential and important part of every AGV based system. The operation ensures that all load consuming stations receive timely service from the AGV. It has to be efficient to achieve the maximum benefits from the system.

The generation of transfer requests is application specific. For autonomous operation of the system, the supervisory controller is required to be connected to plant control system. In that case, the supervisory control system monitors the plant status and combines various requirements in the field efficiently to generate the transfer order requests.

In a semi-autonomous mode, the supervisory system is configured to generate a specific, pre-defined transfer order request based on a set of field status conditions. The supervisory controller module for the AMTS currently works in the semi-autonomous mode. A suitable user interface is provided for the operator to define triggering conditions and corresponding transfer plans to be executed in case the trigger gets activated.

The fully autonomous mode of operation has been analyzed and solution worked out with respect to a specific application environment (automotive sector) and transfer load pattern [5,6]. However, it is difficult to generalize such solutions to other environments.

Display and User Interface

The supervisory controller continuously displays the status of various sub-systems on the control console. The display includes update of the locations of the AGVs in the system, the status of operation of AGV load handling equipment, AGV battery charge status, field conveyors status and the indication of any warnings and faults generated on any of the sub-systems. The controller also provides user interface for manual intervention. This includes the facilities for emergency stopping of the AGV, conveyors etc., in case of any fault on the system. The interface also allows generation and transmission of a manual transfer order to an AGV. The system keeps logging in all the status, warning and fault messages which can be used for generating the statistical data for the system as well as for fault debugging. Fig. 4 shows the Supervisory Control software screen

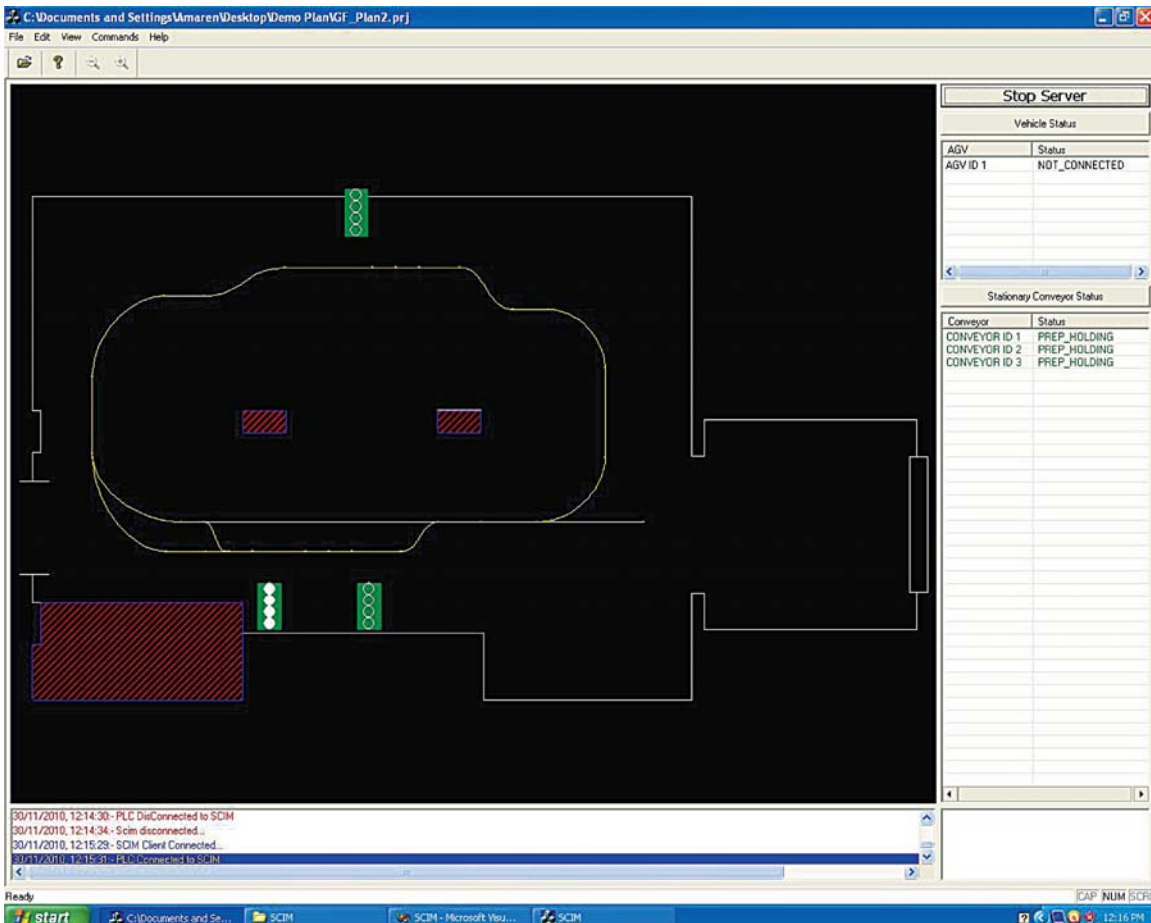


Fig. 4: Supervisory Control Software Screen

during operation of the AMTS. The software depicts the status of the various field devices (conveyors etc). It also dynamically updates the AGV positions on the plan (not shown in the current figure).

Test runs

In order to test, debug and eventually establish integrity of the entire hardware software setup going into the AMTS, we have created a mock material transfer environment in the Ground Floor Hall of our Building. The Hall measures approximately 20m x 10m. We have installed one loading station and two unloading stations on a closed trajectory. Fig. 4 shows the arrangement as shown on the display of the Supervisory Controller. Transfer orders are assigned to the lone AGV in this system by the Supervisory Controller in a way such that the AGV keeps looping around the Hall and keeps transferring

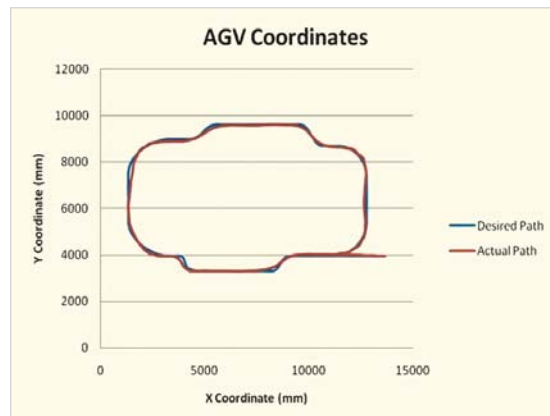


Fig. 5: Path following executed by AGV

in and out stacked bins purportedly carrying materials. While the AGV has no problem in completing loops, there are occasionally problems in material transfer because of level difference between the conveyors.

Fig. 5 shows the desired and actual path followed by the AGV during execution of a material transfer plan. There are small deviations of the actual trajectory from the reference trajectory at several points – particularly at turns, or at places where the motion mode undergoes change. However, it is mainly the errors in position and orientation of the AGV, when it stops for a transfer, that counts, as that affects the reliability of material transfer.

While positioning the AGV for a transfer, errors in alignment, orientation, and distance were measured systematically. It was observed that the errors are well within acceptable limits (± 10 mm for alignment, ± 1 degree for orientation, and 100mm for distance) for autonomous operation of the AGV. While we are keen to reduce the errors, we realise that there is a limit to the precision of control because of limitations of the underlying AGV steering mechanisms (e.g., backlash in steering angles of drive wheels). Moreover, the switching of motion modes (tangential to crab and vice-versa) of the AGV, makes it even more difficult to track the reference trajectory consistently.

Conclusion

We have completed development of the first prototype of an automated material transfer system and demonstrated its operation to potential users and manufacturers. Although a specific application in the automotive sector was picked up as a model for design of the AGV and its control software, the solutions so generated are general enough to be used with modifications or enhancements in other application environments as well. Because of the need for customization, the technology is inherently expensive. It will become affordable to the Industries in the country once solutions are generated locally based on the presented technology. Since the control architecture is modular, a wide range of sensors, navigation and localization systems can be interchangeably interfaced to the system as per availability and requirement.

References

1. Rahul Sakrikar, Sanjeev Sharma, P V Sarngadharan, V K Shrivastava, Vaibhav Dave, Namita Singh, Vikrant Agashe, Biswajit Das, Prabir K Pal, Manjit Singh, "Indigenous Development of an Automated Material Transfer System", National Conference on Robotics and Intelligent Manufacturing Process, Bharat Heavy Electricals Limited, Hyderabad, 2009.
2. SICK NAV-200 & S-3000 series product documents and manuals.
3. Coulter, R.Craig, "Implementation of the pure pursuit path tracking algorithm" (Tech report CMU-RI-TR-9201) Carnegie Mellon University, 1992.
4. Vaibhav Dave, Sanjeev Sharma, Prabir K Pal, "Path Tracking of Mobile Robots with Pure Pursuit Algorithm", National Conference on Robotics and Intelligent Manufacturing Process, Bharat Heavy Electricals Limited, Hyderabad, 2009.
5. Namita Singh, PV Sarngadharan, Prabir K Pal, "AGV Scheduling for Automated Distribution of Materials", National Conference on Robotics and Intelligent Manufacturing Process, Bharat Heavy Electricals Limited, Hyderabad, 2009.
6. Namita Singh, P.V. Sarngadharan, and P.K. Pal, "AGV Scheduling for Automated Material Distribution - A case study", *Journal of Intelligent Manufacturing*, Vol.20, No.4, DOI 10.1007/s10845-009-0283-9, July 2009.

Development of a TB-PCR Kit for the Diagnosis of Tuberculosis

Savita Kulkarni and M.G.R. Rajan

Radiation Medicine Centre

and

Papia Hazra and A. Islam

JONAKI, BRIT

Abstract

More people die of tuberculosis (TB) in India than due to any other infectious disease. The early diagnosis of pulmonary TB (PTB) and extra-pulmonary TB (EPTB) is the most important step that will help in controlling the transmission of TB in the community. As the conventional techniques lack sensitivity, specificity or are too lengthy, it is important to develop a test which is rapid, sensitive and specific. A test based on polymerase chain reaction (PCR) fulfills all these criteria and hence a PCR test was developed at RMC for the rapid diagnosis of tuberculosis. After successful validation of the test, both in PTB and EPTB, and development of an efficient DNA extraction method, a diagnostic kit was developed in collaboration with JONAKI, BRIT. The kit, now launched in the market, will be useful in early diagnosis of TB.

Introduction

Tuberculosis caused by *Mycobacterium tuberculosis* (MTB), is a public-health problem of global importance. According to the World Health Organization, more than 8 million people develop TB each year. In the last decade, TB has reemerged as one of the leading causes of death, killing nearly 3 million people annually. India holds one-fifth of the global burden of TB with more than 350,000 deaths every year. The emergence of HIV infection and a rising prevalence of multi-drug resistant (MDR) tuberculosis have threatened the effectiveness of standard chemotherapy such as Directly Observed Treatment (DOTS). Though, most of the total TB population is contributed by PTB, almost 10-15% of total cases are EPTB.

An aspect of tuberculosis control that clearly needs improvement is the speed with which the diagnosis is confirmed. This is especially true with pulmonary tuberculosis, as these patients are responsible for the respiratory transmission of tuberculosis. Though

the conventional method, AFB smear microscopy, has high positive predictive value, it lacks the sensitivity because of requirement of at least 10^4 bacilli in the spectrum sample for positivity. Culture technique is sensitive and is considered to be the Gold standard, but is labour intensive and takes 3-6 weeks because of extremely slow growth rate due to long generation time (12-18 hr) of mycobacteria. Tuberculin test is another widely used supportive diagnostic test that lacks specificity whereas serological test were found to be unsatisfactory both in sensitivity and specificity⁽¹⁾.

The invention of Polymerase Chain Reaction (PCR), a Nobel Prize winning technology by Kary Mullis (1993) finally provided an exciting boost in the diagnosis of tuberculosis. As this technique offered amplification of small amount of DNA it was extensively evaluated for the detection of MTB from clinical samples¹. A number of published reports have exhibited quite good sensitivities and specificities for the detection of MTB from sputum samples for the diagnosis of PTB.

Many of the PCR tests for *MTB* detection, described in the literature, are based on amplification of *IS6110* sequences that is believed to be restricted to members of the *MTB* Complex³. The presence of multiple copies of this element in the majority of *MTB* strains undoubtedly enhances the sensitivity of PCR. The discovery of occasional *MTB* strains

lacking *IS6110* in India⁴ however implies the possibility of a few false negative results in the test with *IS6110*-based PCR. To overcome these problems, a PCR test was developed in our laboratory targeting a house keeping gene of *MTB* for the 38 kDa protein, involved in phosphate transport⁵.

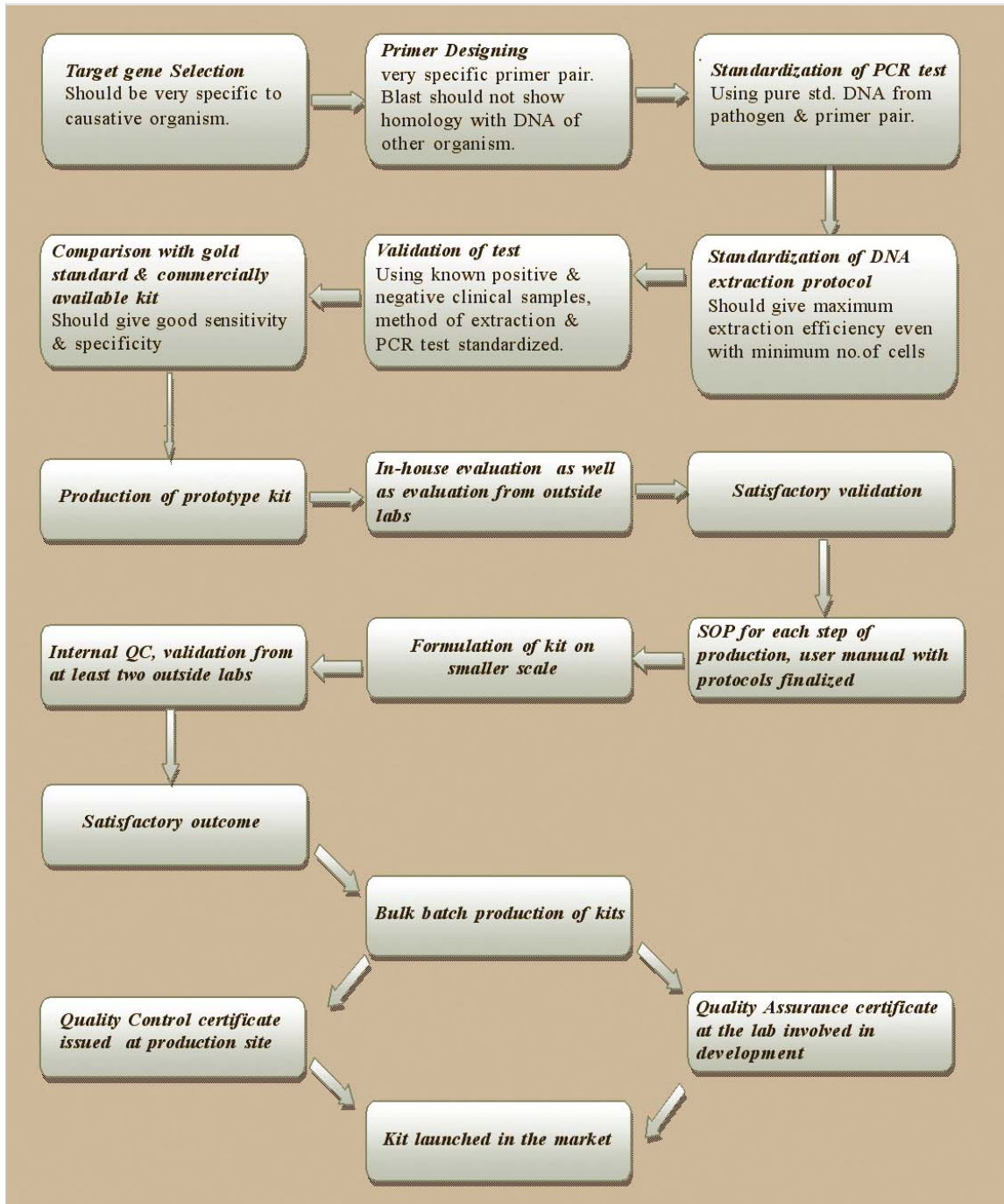


Fig. 1: Development of TB PCR kit- Steps involved

The PCR conditions were optimized using standard MTB DNA. The analytical sensitivity and specificity of the test were established. Different DNA extraction protocols were standardized and compared for extraction efficiency. Standardized protocols were then used on clinical samples such as sputum from pulmonary TB cases and abdominal biopsies and Cerebro Spinal Fluids from patients with extra-pulmonary TB for validating the PCR test. After satisfactory validation, it was decided to the test market, in a kit form, jointly by RMC and JONAKI, BRIT. The flow chart in Fig. 1 illustrates various steps involved in development and commercialization of TB-PCR kit.

Methods

A) Standardization of PCR test

A primer pair KD1 and KD2 (KD1 5' – CCAAGCAAGATCCCGAGGGCT – 3', KD2 5' – TTG-ATG-ATCGGGTAGCCGTCC – 3'), targeting 340bp segment of the 38kDa gene of *MTB* was designed and blast search was performed to confirm its specificity. PCR was standardized using the primer pair and DNA from a standard strain, *MTB* H37Rv,

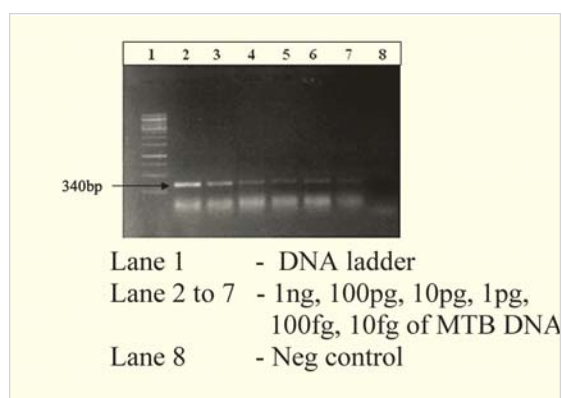
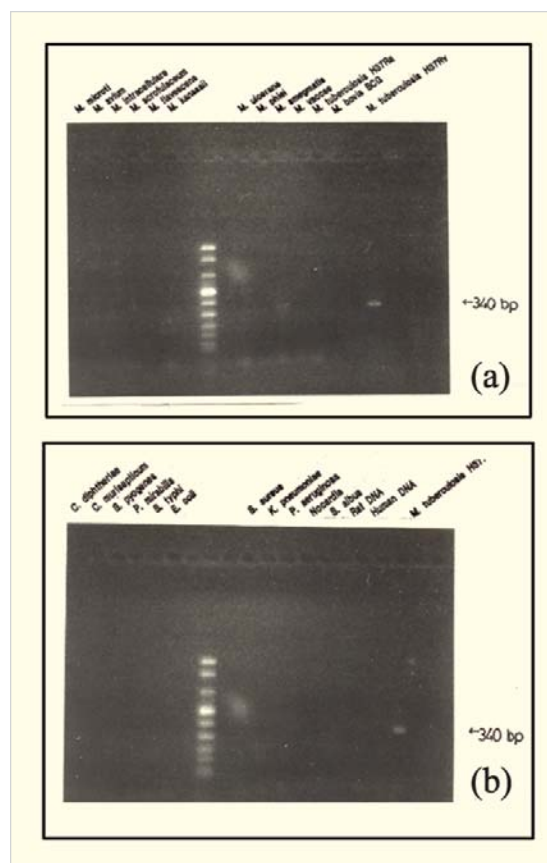


Fig. 2: Sensitivity of KD1 and KD2 PCR test

grown in laboratory. The analytical sensitivity of the PCR test was found to be 10fg which is equivalent to 3 bacilli (Fig. 2). The test was proved to be specific only to *MTB* complex strains and



- Amplification and hybridization with DNA from various non-TB mycobacteria.
- Amplification and hybridization with DNA from bacteria other than mycobacteria, human DNA and rat DNA

Fig. 3: Specificity of KD1 and KD2 PCR test

did not give amplification with various bacterial DNA as well as human DNA (Fig. 3).

B) PCR test validation for pulmonary as well as extra-pulmonary tuberculosis

The PCR test was validated for PTB (168 sputum samples from TB patients) as well as EPTB (50 abdominal biopsies from suspected abdominal TB cases and 60 CSF samples from TB meningitis cases). The DNA was extracted using phenol-chloroform method for sputum samples and abdominal biopsies whereas only proteinase K with boiling treatment was used for CSF samples. The test was always performed in duplicate and one of

the test samples was spiked with positive control DNA to look for the inhibition. Amplicons were visualized in ethidium bromide stained agarose gel. For CSF samples the sensitivity was further increased using Southern hybridization and ECL detection using biotinylated internal probe whereas dot-blot hybridization was performed for abdominal biopsies using radioactive internal probe.

Various procedures for extracting DNA from clinical samples were evaluated for their extraction efficiency and ability to remove inhibitors. QIAGEN® column extraction method with modifications was found to be the most satisfactory procedure. This extraction protocol was again validated for PTB (sputum samples, n=72). The promising results led to production of a silica column based indigenous TB-PCR prototype kit jointly by RMC and JONAKI, BRIT. The prototype kit was again validated using 110 sputum samples from PTB patients and 72 samples from healthy controls.

Results

Clinical Evaluation

Initial validation of the standardized PCR test performed with 168 sputum samples exhibited 77% positivity in smear positive samples and 10 % sample showed PCR inhibition. (Table 1a). Study and abdominal biopsies showed sensitivity and specificity

of 77% and 68% respectively⁶ (Table 2a). The detection of the amplicons was very difficult due to presence of large amount of human DNA in PCR reaction; hence the results were confirmed after dot blot hybridization with radioactive internal probe wherever required. In the double-masked study of Tuberculous meningitis (TBM) patients, 73.3% sensitivity observed with ethidium bromide staining was increased to 90%⁷ (Table 2, b) by using Southern hybridization and Enhanced Chemiluminescent (ECL) with biotinylated internal probe.

Evaluation of silica column based extraction procedure and prototype kit

PCR test performed with DNA extracted from 72 sputum samples using QIAGEN® silica column extraction method, exhibited 87% positivity in culture positive samples with none showing PCR inhibition. Further, 40% clinically diagnosed TB patients also could be detected by the PCR test (Table 1b).

The prototype kit produced jointly by RMC and JONAKI, BRIT when evaluated using clinical samples from TB patients and non-TB controls, showed sensitivity of 84% and specificity of 97%. (Table 3). A small batch of kits was then produced and the kits were given to different hospitals for evaluation.

Table 1: Evaluation of PCR test for pulmonary tuberculosis targeting 38kDa protein gene using KD1 and KD2 primers

Clinical samples	DNA Extraction Method	AFB/CultureStatus (Number)	PCR Pos (%)	PCR Inhibition(%)
a) Sputum from TB patients (N=168)	Phenol-chloroform	Pos/Pos (N=36) Neg/Pos(N=50) Neg/Neg (Clinically diagnosed) (N=82)	28 (77%) 28 (56%) 19 (22%)	2(5.5%) 7(14%) 9(10.9%)
b) Sputum from TB patients (N=76)	QIAGEN silica column method	Pos/Pos (N=14) Neg/Pos(N=17) Neg/Neg (Clinically diagnosed) (N=45)	14 (100%) 13 (76%) 18 (40%)	(0%) (0%) 0(%)

Table 2: Evaluation of PCR test for extra- pulmonary tuberculosis targeting 38kDa protein gene using KD1 and KD2 primers

a) Abdominal tuberculosis*⁽¹¹⁾							
Clinical samples	DNA Extraction Method	Clinical diagnosis	PCR Pos (%)	SEN.	SPE	PPV	NPV
Laparoscopic abdominal biopsies	Phenol-chloroform	†HP pos (N=31) HPNeg (N=19)	24(77%) 6(31.5%)	77%	68.5%	80%	73%

b) Tuberculous meningitis (TBM)^{♦(12)}							
Clinical samples	DNA Extraction Method	Clinical diagnosis	PCR Pos (%)	SEN.	SPE	PPV	NPV
CSF	Proteinase K treatment and boiling	TBM (N=30) Controls(N=30)	27(90%) 0 (0%)	90%	100%	100%	97%

* Abd. TB. -Amplicon detection by southern hybridization with ³²P labeled internal probe
† HP- histopathology. HP was used as gold standard ,
♦ TBM- Amplicon detection by biotin labeled internal probe and ECL detection.

Table 3: Validation of BRIT-RMC PCR kit for detection of M.tuberculosis

Total No. Sputum samples From TB patients (N=110)	BRIT- RMC kit- PCR positives *(%)
Smear +ve & Culture +ve (N=64)	54 (84.3%)
Smear -ve & Culture +ve (N=19)	10 (52.3%)
Smear -ve & Culture -ve (N=37)	8 (21.6%)
Controls (Non-TB patients) N=72	3 (2.7%)

After a satisfactory feed-back, a bulk production was carried out and a totally indigenous kit which contains both column based DNA extraction as well as PCR reagents was launched in the market in Aug 2009 by BRIT, BARC Fig. 4 a & b.

Discussion

TB-PCR fulfills all the criteria required for being an ideal diagnostic test, in comparison to existing tests for early detection of TB and, hence, justifies being the test of choice. PCR is theoretically capable of amplifying even a single copy of DNA. Further, all types of biological specimens such as sputum, blood, bronchoalveolar lavage, CSF, biopsies, pleural and ascitic fluid are amenable to PCR analysis and, hence, it has been proved to be the successful technique for identification of numerous pathogens in various biological specimens. Thus adaptation of PCR for detection of MTB in uncultured clinical specimens has revolutionized TB diagnosis.

The first target used in for PCR for diagnosis of TB, was a 65 kDa heat shock protein of MTB⁸, but showed cross reactivity due to the conserved nature of this gene throughout all living organisms. Subsequently specific targets for PCR like the antigen 85 complex⁹ and *IS6110*³ were evaluated, which

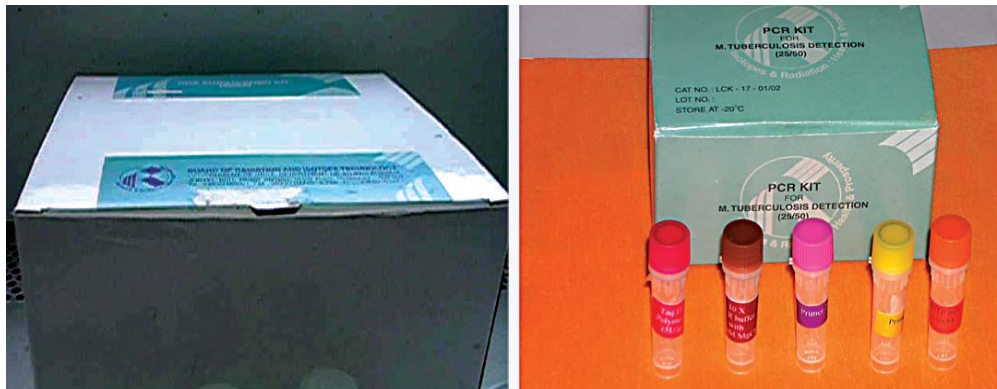


Fig. 4: Indigenous TB-PCR kit jointly produced by RMC and BRIT
a) DNA extraction kit b) PCR reagents kit

illustrated good sensitivities and specificities. Our target also showed a very high sensitivity and specificity proving its usefulness. The elimination of inhibitors is one of the most difficult challenges in the diagnostic PCR test. Thus, DNA extraction procedure yielding pure and clean DNA from clinical specimens is the key to the success of PCR. Use of silica membrane in the kit was observed to have great efficacy for removing Taq polymerase inhibitors from blood, sputum and other biological material and hence, no inhibition of PCR and no false negativity was seen. Our studies also emphasized the fact that we may need to use appropriate extraction and amplicon detection methods for different clinical samples.

Clinical evaluation

Pulmonary tuberculosis: As per the recent meta-analysis by Greco et al¹⁰ the diagnostic sensitivity and specificity of different PCR tests for smear positive respiratory samples varied among different laboratories and was in the range of 80-95%. Our prototype kit could detect 84% smear and culture positive cases. Additionally, our test could also detect 52% of smear negative but culture positive TB cases and 22% of smear and culture negative TB cases, which is considered to be a challenge in TB diagnosis.

Tuberculous meningitis: TBM is one of a common clinical manifestation of EPTB which can

be fatal. Definitive diagnosis is not possible as smear and culture are rarely positive and in the absence of gold standards, a PCR test like ours with 90% sensitivity will be very useful in the early diagnosis of TBM and this will further help in decreasing the rate of mortality.

Abdominal tuberculosis: It is an important EPTB which is difficult to diagnose due to the diagnostic dilemma in histopathology. When AFB and culture are negative, PCR is the only reliable technique that can confirm the presence of *MTB* in the affected site and further help in ruling out malignancy. Ours is one of the very few studies that were done on fresh laparoscopic abdominal biopsies which showed reasonably good sensitivity and specificity.

RMC, BARC and JONAKI, BRIT have successfully developed an inhouse TB-PCR test for both pulmonary and extra-pulmonary tuberculosis and have made it commercially available after different levels of quality evaluation and validation.

References

1. Shinnick TM, Jonas V. "Molecular approaches to the diagnosis of tuberculosis". In Bloom BR ed. Tuberculosis : Pathogenesis, protection and control. Washington DC, American Society for Microbiology Press, 1994: 517-530.

2. Kadival GV, D'Souza CD, Kolk AHJ, Samuel AM. "Polymerase chain reaction in the diagnosis of tuberculosis comparison of two target sequences for amplification". *Zbl. Bakt.* 282 (1995): 353-361.
3. Caws M, Wilson SM, Clough C, Drobniewski F. "Role of IS6110 Targeted PCR, culture biochemical clinical and immunological criteria for diagnosis of tuberculosis meningitis". *J. Clin. Microbiol.* 38 (2000) : 3150-3155.
4. Van Soolingen D, DeHaas PEW, Hermans PWM, Groenen PMA, van Embden JDA. "Comparison of various repetitive DNA elements as genetic markers of strain differentiation of epidemiology of *Mycobacterium tuberculosis*". *J. Clin. Microbiol.* 31 (1993) : 1887-1895.
5. Harboe M and Wiker HG. "The 38 kDa protein of *Mycobacterium tuberculosis* : A review". *J. Infect. Dis.* 166 (1992): 874-884.
6. Kulkarni SP, Jalil MA, Kadival GV. "Evaluation of polymerase chain reaction for the diagnosis of tuberculous meningitis in children". *J Med Microbiol.* 54 (2005):369-373.
7. Kulkarni SP, Vyas SP, Kadival GV. "Use of Polymerase chain reaction in the diagnosis of abdominal tuberculosis". *J Gastroenterol and Hepatol.* 21 (2006) : 819-823.
8. Pao CC, Yen B, You JB, Maq JS, Fiss EH and Chang CH. "Detection and identification of *Mycobacterium tuberculosis* by DNA amplification". *J. Clin. Microbiol.* 28 (1990) : 2200-2204.
9. Fauville-Duafaux M, Vanfleteren B, Dewil L, Unckle JP, vanVooren JP, Yates MD, Serruys E and Content J.: Rapid detection of tuberculous and non-tuberculous mycobacteria by polymerase chain reaction amplification of a 162 bp DNA fragment from antigen 85. *Eur. J. Clin. Microbiol. Infec. Dis.* 11(1992) : 797-803.
10. Greco S, Girardi E, Navarra A, and Saltini C. "Current evidence on diagnostic accuracy of commercially based nucleic acid amplification tests for the diagnosis of pulmonary tuberculosis". *Thorax.* 61 (2006) :783-790.

Report on 3rd AONSA Neutron School held at BARC

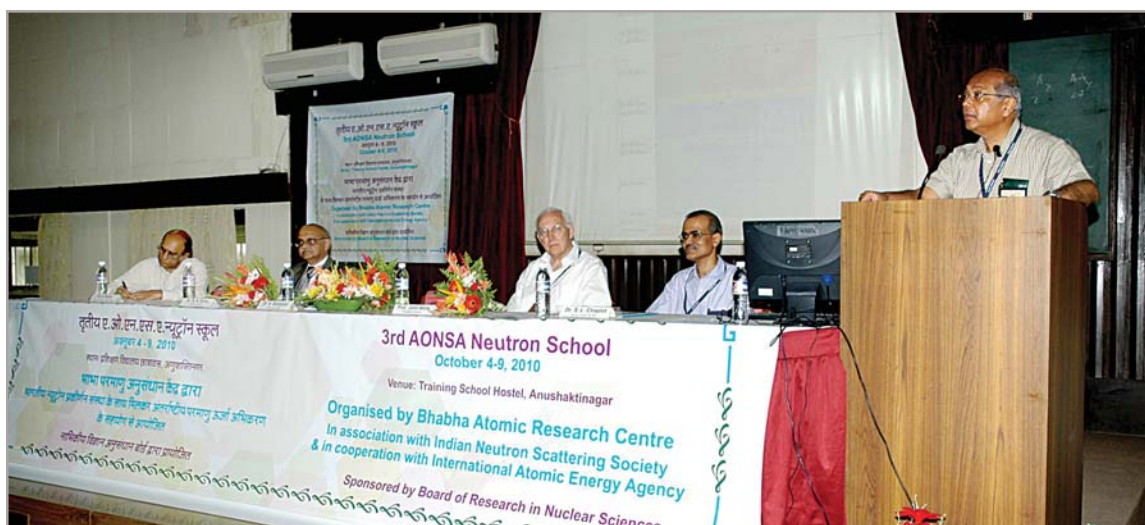
BARC operates a National Facility for Neutron Beam Research at the Dhruva reactor. The National Facility is regularly utilized in collaboration with about 200 users from various universities and other academic institutions. At present there are over 25 active projects under the universities (UGC-DAE-CSR) collaboration programme. BARC has been regularly organizing Schools on neutron scattering in cooperation with UGC-DAE-CSR, often including hands-on experiments at Dhruva.

The 3rd Asia Oceania Neutron Scattering Association (AONSA) Neutron School was held at BARC, Mumbai during October 4-9, 2010. This follows the previous AONSA Neutron Schools at Korea (2008) and Australia (2009). The present School was sponsored by Board of Research in Nuclear Sciences, Department of Atomic Energy, Government of India. It was organized in association with Indian Neutron Scattering Society and in cooperation with IAEA. The School covered various aspects of neutron

scattering instrumentation, research and applications in physics, chemistry, biology, and material science.

The distribution of the student participants was: Australia and New Zealand (5), India (19), Japan (2), Indonesia (3), Korea (3), Taiwan (5), and Malaysia (1). Theory lectures were delivered during the first three days of the School by 7 Indian and 6 foreign scientists. This was followed by two days of hands-on experiments that were conducted by the respective instrument scientists at the Dhruva reactor at BARC. On the last day of the school, 14 students made oral presentations of their research work.

During the feedback session, the students expressed their satisfaction and thanked all the contributors. Generally the students appreciated the broad introduction to various techniques that would be very useful and the interactions during the experiments.



Dr. S. Banerjee, Chairman, AEC giving his address at the inaugural function on Oct. 4, 2010. On the dais (L to R): Dr. S. Kailas, Director, Physics Group, BARC, Dr. R.K. Sinha, Director, BARC, Dr. John White, President AONSA and Dr. S.L. Chaplot, Coordinator, 3rd AONSA Neutron School

55th DAE Solid State Physics Symposium (SSPS)2010: a report

The 55th DAE-Solid State Physics Symposium (SSPS) was held at Manipal University, Manipal during Dec. 26-30, 2010. Dr. R. Mukhopadhyay, SSPD, BARC, was the convener of the symposium and Dr. Alka Garg, HP&SRPD and R. Mittal, SSPD, BARC were the scientific secretaries. Prof. Ajay K. Sood, President, Indian Academy of Sciences, inaugurated the symposium and Prof H. Vinod Bhat, Pro Vice Chancellor presided over the inaugural function.

This symposium, sponsored by Board of Research in Nuclear Sciences, Department of Atomic Energy, Government of India, is an annual event. This annual symposium is the largest gathering of solid state physicists in the country. This year the number of contributed papers was received beyond 1100. A panel of experts chosen from various institutes and universities across the country reviewed all the papers. After evaluation, 779 papers were accepted for presentation. The number of registered participants was 860 and 610 contributed papers were presented in the poster sessions, out of which 48 papers were also presented in the oral sessions.

The highlights of the symposium were the inclusion of three theme seminars, 1) Graphene: Paradigm of Exciting Nanophysics, 2) New age Pnictide Superconductor and 3) Materials for Renewable Energy. In addition to these, there were 17 invited talks on

subjects of current interest like multiferroics, nanomaterials, superconductors, novel magnetic materials, disordered and liquid crystals, condensed matter under negative pressure, etc. by eminent scientists from India and abroad. In addition, there were number of contributed papers on similar topics.

An Evening talk "Scientific outlook into ayurveda" was delivered by Prof. M. S. Valiathan. Three researchers were selected for Young Achievers Awards. Three awards were given both in the PhD thesis and in M. Sc project categories and twenty posters were chosen for "Best Poster" awards. A summary of the symposium was presented by Prof A. Ghoshray, SINP, Kolkata in the concluding session. The American Institute of Physics will publish the proceedings of the symposium.



Inauguration of the 55th DAE-SSPS at Manipal University, Manipal. In picture from left: Prof A.K. Sood, President, IASc, Bengaluru, Prof. H.Vinod Bhat, Pro Vice Chancellor, Manipal University, Prof S.L. Chaplot, Head, SSPD, BARC, Prof. R. Mukhopadhyay, Convener, DAE-SSPS 2010, and Prof Ashok Rao, Convener, Local Organising Committee, DAE-SSPS 2010.

Report on DAE-BRNS Symposium on Nuclear and Radiochemistry

The tenth biennial symposium on “Nuclear and Radiochemistry” (NUCAR-2011), organized by the Board of Research in Nuclear Sciences (BRNS), Department of Atomic Energy, in association with the GITAM Institute of Science, Visakhapatnam, and Indian Association of Nuclear Chemists and Allied Scientists, Mumbai, was held during February 22-26, 2011. This conference was exclusively dedicated to nuclear chemistry, chemistry of actinides & fission products and various aspects of radiochemistry. The conference was attended by nearly 350 delegates including scientists from National Laboratories, Universities and Research Institutes from India and abroad.

Inaugurating a five-day biennial symposium at GITAM University, Prof. Rama Rao, Chairman, Board of Research in Nuclear Sciences (BRNS) of Department of Atomic Energy, stressed the need for trained and efficient human resources for making country’s nuclear programmes successful. He said, India’s nuclear programmes are self sufficient and our scientists are capable of handling challenges. Nuclear science and technology should be promoted and awareness must be created among people about radiation and the usefulness of nuclear power. While talking about research activity, Prof. Rama Rao said that BRNS was continuously supporting research programmes of various universities and institutions



NUCAR-2011 Inauguration function, from left to right: Prof. Rama Rao, Chairman, Board of Research in Nuclear Sciences (BRNS), Dr. M.V.V.S. Murthi, President, GITAM University, Prof. V. Venugopal, Director, Radiochemistry & Isotope Group, BARC, Prof N. Lakshmana Das, Principal, GITAM Institute of Science, Dr. R.M. Sawant, Convener, NUCAR-2011, Dr. S.K. Sali, Secretary, NUCAR-2011 and Prof. G. Subramanyam, Vice-Chancellor of GITAM University.

through its various schemes. The top DAE official had a word of praise for Indian universities, particularly deemed universities, who have the benefit of autonomy, and advised them to take reputed US universities as benchmark to improve their quality. He appreciated GITAM University for achieving "A" status among other universities. Prof. Rama Rao hoped that the upcoming Bhabha Atomic Research Centre's unit in Visakhapatnam would be a suitable place to train the required manpower in the nuclear sector.

Speaking on the occasion, Prof. V Venugopal, Director, Radiochemistry & Isotope Group, Bhabha Atomic Research Centre (BARC) said India has a flourishing and largely indigenous nuclear power programme and expects to have 20,000MW nuclear capacity by 2020 and 40,000 MW by 2032. To strengthen the country's co-operation with the international community in the areas of advanced nuclear energy systems, Indian government is establishing a Global Centre for Nuclear Energy Partnership at New Delhi and establishing a Neutron Observatory at Madurai to strengthen nuclear physics research activities.

GITAM University president Dr. M.V.V.S.Murthi lamented that students preferred IT and other courses to basic sciences. To make youngsters join science courses, incentives must be provided. Vice-chancellor of GITAM University Prof. G Subramanyam briefed about the university's teaching and research activities. He expressed that the university is interested to offer nuclear technology programs under the guidance of DAE and other organisations. Principal, Institute of Science Prof N. Lakshmana Das, Symposium organizing committee, Convener, Dr. R.M. Sawant, Secretary Dr. S.K. Sali, IANCAS General Secretary, Dr. A.V.R Reddy and GITAM UGC Affairs Director, Prof. Ramakrishna participated in the inaugural session.

A special seminar was arranged to commemorate the centenary of the discovery of atomic nucleus by Ernest Rutherford, during this symposium. Prof. Marshall from Rutherford's laboratory gave an invited talk on the birth of atomic nucleus and highlighted the contributions of Rutherford.

Indian Association of Nuclear Chemists and Allied Scientists (IANCAS) felicitated and presented two life time achievement awards to noted scientists Dr. R.H. Iyer, Former Head, Radio Chemistry Division, BARC with M. V. Ramaniah award and Dr. S.V. Narasimhan, Former Assoc. Director, Chemistry Group, BARC, with the Dr. K.S. Venkateshwarlu award.

National Symposium on Advanced Measurement Techniques and Instrumentation (SAMTI-2011): a report

The first National Symposium on Advanced Measurement Techniques and Instrumentation (SAMTI-2011), sponsored by DAE-BRNS and in association with Indian Physics Association (IPA), was held at the Multipurpose Hall, Training School Hostel, Anushaktinagar, Mumbai during 2-4, February 2011. Over three hundred delegates from major scientific, academic and industrial organizations from India and three experts from Denmark, France and Switzerland, participated in this symposium. A salient feature of the symposium were the 25 invited lectures, delivered by eminent speakers from India and abroad and 62 contributed papers covering a wide spectra of topics in measurement of science and technology.

The symposium was inaugurated by Dr. S. Banerjee, Chairman, AEC and Secretary, DAE in the august presence of Dr. S. Kailas, Director, Physics Group and President, IPA and the Guest of Honour Shri G.P. Srivastava, Director, E&I Group. Dr. S. Banerjee emphasized the importance of the role played by scientists and engineers in developing innovative measurement techniques and transforming them into making of appropriate instruments. The Inaugural session was concluded with a scintillating key note address on "Measuring the Unseen and Unfelt Phenomenon" by Prof. E.S.R. Gopal, IISc, Bengaluru.



Dr. S. Kailas (Director, Physics Group and President IPA) addressing delegates during inaugural function of SAMTI-2011. (L-R) Dr. S. V. G. Ravindranath (Convener, SAMTI-2011), Shri G.P. Srivastava (Director, E&I Group and Guest of Honor), Dr. S. Banerjee (Chairman, AEC and Secretary, DAE), Dr. B. N. Jagatap (Chairman SAMTI-2011) and Shri R. Sampathkumar, Secretary, SAMTI-2011

The technical programme of the symposium consisted of 8 thematic sessions and two poster sessions devoted to Measurement and Instrumentation in Physical Sciences, Extreme Environments, Chemical and Biological Sciences, Astronomy and Remote Sensing, Accelerators and Beamline Diagnostics and Mathematical Techniques. The galaxy of speakers included Prof. P. Banerjee, NPL, New Delhi (Importance of quantum standards in precise measurement), Dr. R.C. Naik, UEPL, Vapi (Indigenous development of instruments for air and pollution measurements), Prof. V. Ramgopal Rao, IITB, Mumbai (Nano-electro-mechanical systems for health care and security applications), Prof. Soumyo Mukerji, IITB, Mumbai (Evanescent wave optical biosensors), Prof. S. Ananthkrishnan, Pune University, Pune (Modern radio astronomy instruments with high SNRs and high resolution), Shri. S. Bhattacharya, Asso. Director(T), E&I Group, BARC (Development of time domain electromagnetic system), Prof. S.K. Saha, IAP, Bengaluru (Optical Instrumentation for telescopes: Interferometry with or without real time corrections), Dr. J.S. Nielsen, Aarhus University, Denmark (The diagnostic systems for ASTRID and ASTRID2), Prof. R. Pillay, TIFR, Mumbai (Instrumentation for the heavy ion super conducting LINAC at TIFR), Dr. Vinod Chohan, CERN, Geneva (Super conducting magnet tests and measurements for LHC), Dr. L. Nahon, SOLEIL, France (All about DESIRS: A VUV high resolution variable polarization beamline at SOLEIL for dichroism and spectroscopy), Dr. B. Satyanarayana, TIFR (Detector R&D for INO project), Dr. Amar Sinha, BARC (Neutron and X-ray based diagnostic techniques), Dr. R. Nagendran, IGCAR, Kalpakkam (SQUID sensor and its applications), Shri Nirbhay Gupta, NPCIL, Mumbai (Condition monitoring system for rotary machines), Shri P. Phatnani, RRCAT, Indore (EPICS based control and data acquisition in accelerators), Dr. Ayan Ray, VECC, Kolkata (Advanced instrumentation in laser spectroscopy: from ultras to extremes), Prof. Ratneshwar Jha, IPR,

Gandhinagar (Measurement in harsh environment of fusion plasma), Dr. S. Sendhil Raja, RRCAT, Indore (MOEMS technology in laser based instrumentation), Prof. Shankar Narasimhan, IITM, Chennai (Development of multivariate calibration models for noisy spectral data), Prof. Ravindra Gudi, IITB, Mumbai (A tutorial overview of different methods to remove noise from the measurements), Prof. Arun Tangirala, IITM, Chennai (Application of matrix factorizations to data analysis- An overview) and Prof. Mani Bhushan, IITB, Mumbai spoke (Data reconciliation as a tool to enhance sensor performance). The program also included an evening talk by Dr. B.A. Dasannacharya, Mumbai on "Wanderings in the Garden of Measurements". The concluding session featured an illuminating talk by Dr. S.K. Sikka, Homi Bhabha Chair Professor, DAE on "Status of instrument development in India".

Participants expressed their appreciation over the topics covered by eminent speakers, their interaction with industries participated in the industrial exhibition and echoed the opinion expressed in the inaugural session that this symposium should be conducted bi-annually.

3rd DAE-BRNS International Symposium on Materials Chemistry (ISMC – 2010): a report

The 3rd DAE-BRNS International Symposium on Materials Chemistry (ISMC-2010) organized by the Chemistry Division and Society for Materials Chemistry, was held at BARC during 7-11 December, 2010. The symposium programme comprised 35 invited talks and more than 450 contributed papers covering frontline research in diverse areas of Material Science such as Nuclear Materials, Fuel Cell Materials, Nanomaterials, Thin Film Devices and Sensors, Hydrogen Storage Materials, Magnetic Materials, Catalysts, Polymers, Carbon based Materials, Organic Materials etc. The deliberations focused on materials research programmes for harnessing power from nuclear fission, fossil fuels, hydrogen and other sources. The development of new technologies based on nanomaterials for the above applications e.g. in separation science was

discussed at large. Eminent Scientist, Prof. C.N.R. Rao, FRS (Padma Vibhushan), in his keynote address, highlighted the importance of advanced materials in emerging technologies. In particular, he emphasized on graphene, which is emerging as an excellent multifunctional material.

Dr. S. Banerjee, Chairman, Atomic Energy Commission delivered a very lucid special evening lecture on "Phase transformations in solids: A scheme for classification". Prof. A.K. Cheetham, FRS, delivered a talk on "Inorganic–Organic Framework Materials". Other speakers from India and abroad gave invited talks on a variety of topics such as defects chemistry of fluorite type materials, high pressure studies, synthesis of metal hydrides, nanomaterials, catalysis, SANS/SAXS characterization



From left to right: Dr. S.K. Kulshreshtha, Chairman, AEES, Dr. Tulsi Mukherjee, Director, Chemistry Group, Prof. C.N.R. Rao, FRS Honorary Director, JNCASR, Bengaluru, Prof. A.K. Cheetham, FRS, Cambridge University, UK, Dr. J.P. Mittal (M.N. Saha Distinguished Fellow) and Dr. D. Das, Head, Chemistry Divn.

of food materials, actinide oxides, hypervalent urania, boron dipyrromethane, organic semiconductor films, inorganic-organic hybrid materials, theoretical modeling as well as experimental studies on solar cell absorbers, metal chalcogenides, materials for environment, negative thermal expansion materials, nano-fluids, multi-layers, thin films, radiation induced modification of polymeric materials and many other topics in materials chemistry.

In the 5-day long deliberations, 20 scientists from USA, Russia, Sweden, France, Germany and Canada, and 15 scientists from our national research centres, IITs and Universities made invited presentations of their recent work. About 450 poster presentations on four consecutive days (7-10 December, 2010) were well attended. Seven Best Posters were selected for awards by expert committees. Valedictory session on the 11th December, 2010 was presided over by Dr. T. Mukherjee, Director, Chemistry Group. Dr. A.K. Suri, Director, Materials Group was the chief guest of the valedictory function.

Forthcoming Conference

21st International Conference on Structural Mechanics in Reactor Technology (SMiRT-21)

SMiRT-21 will be held at the India Habitat Centre, New Delhi, India, from 6-11 November, 2011.

This conference will be dedicated to the Art, Science and Practice of Structural Mechanics. It will aim to cover all technical and professional practice issues, relevant to Structural Mechanics in Reactor Technology. Around 800 delegates are expected to attend this Conference, which will have 8-10 parallel sessions every day.

A technical exhibition for displaying various technologies and products will be held during SMiRT-21. The exhibition will remain open during the entire period of the Conference.

For further details. One may contact:

B.K. Dutta

Chairman, SMiRT-21.

Reactor Safety Divn.,

Bhabha Atomic Research Centre,

Trombay, Mumbai-400 085, INDIA

Email: smirt21@hbni.ac.in

Tel: 91-22-25593778 (O)

91-22-25527668 (R)

Fax: 91-22-25505151

BARC Scientists Honoured

Name of the Scientists : **Rajendran Menon, Anindya Chakravarty, Mukesh Goyal, Mohananand Jadhav, Arun S., Satish Kumar Bharti and Trilok Singh**
Cryo-Technology Division

Title of the paper : High Speed Cryogenic Turboexpander Rotor for Stable Operation upto 4.5 kHz Rotational Speed

Award : Best Paper Award

Presented at : 23rd National Symposium on Cryogenics (NSC-23) held at NIT, Rourkela, during October 28-30, 2010

Name of the Scientists : **S.V. Ingale, Ratanesh Kumar, J.K. Singh, R.P. Patel, P.B. Wagh and Satish C. Gupta**
Applied Physics Division

Award : 1st prize for the Best Poster presentation

Presented at : National Seminar on Physics of Materials and Materials Based Device Fabrication (NSPM-MDF-2011) organized by Department of Physics, Shivaji University, Kolhapur, during February 17-18, 2011

Name of the Scientists : **Rajalaksmi R., G.J. Gorade, B.S.V.G.Sharma and P.K. Vijayan**
Reactor Engineering Division

Title of the paper : "Development of Sensor Instrumentation for Void and Two-Phase Mass Flux Measurements in High Pressure Steam-Water Application"

Award : Best Oral Presentation Award

Presented at : "National Seminar on Physics and Technology of sensors (NSPTS-16)" held at Department of Physics, University of Lucknow, Lucknow, during February 11 - 13, 2011.

Name of the Scientists : **G.J. Gorade, Rajalaksmi R. and B.S.V.G. Sharma**
Reactor Engineering Division

Title of the paper : "Signal analysis techniques using DSP for flow regime identification in two phase flow"

Award : Best Poster Award

Presented at : National Symposium on "Advanced Measurement Techniques and Instrumentation (SAMTI-2011)" held at Bhabha Atomic Research Centre, Anushaktinagar, Mumbai, during February 02-04, 2011.

Name of the Scientists : **D.K. Koul and P.G. Patil**
Astrophysical Sciences Division

Title of the paper : "High temperature thermally transferred optically stimulated luminescence phenomenon - feasibility in dose estimation of Ceramics"

Award : Best Poster Award

Presented at : National Conference on Luminescence and its Applications held at Pt. Ravishankar Shukla University, Raipur, during Feb.7-9, 2011.



Sandalwood Tree

Edited & Published by :
Dr. K. Bhanumurthy,
Head, Scientific Information Resource Division,
Bhabha Atomic Research Centre, Trombay, Mumbai 400 085, India.
Computer Graphics & Layout : N. Kanagaraj and B. S. Chavan, SIRD, BARC
BARC Newsletter is also available at URL: <http://www.barc.gov.in>